Simultaneous Determination of Pyridine-Triphenylborane Anti-Fouling Agent and Its Degradation Products Using Capillary Zone Electrophoresis

KAEWCHUAY, NETNAPIT

(Degree)
博士（学術）

(Date of Degree)
2013-03-25

(Date of Publication)
2013-09-05

(Resource Type)
doctoral thesis

(Report Number)
甲5803

(URL)
https://hdl.handle.net/20.500.14094/D1005803

Doctoral Dissertation

Simultaneous Determination of Pyridine-Triphenylborane Anti-Fouling Agent and Its Degradation Products Using Capillary Zone Electrophoresis

キャピラリーゾーン電気泳動法によるピリジントリフェニルボラン防汚剤及び分解生成物の同時定量

January 2013

Graduate School of Maritime Sciences

Kobe University

Netnapit Kaewchuay

CONTENTS

General Introduction

Pyridine-Triphenylborane (Anti-fouling agent)

The fouling results from the growth of marine organisms, such as barnacles, mussels, tubeworms, and algae, on the surface of ship hulls leads to reduction of speed, increased fuel, maintenance costs, damage of ship hulls and platform, and losses in the time. [1, 2]. Therefore, anti-fouling coating that contains the biocide are used and applied to ship hulls to prevent the growth of their organisms. Many kinds of compounds have been used as biocides in anti-fouling agents. The history for using the anti-fouling agents is summarized by Omae [3]. Tributyltin (TBT) compounds, anti-fouling agent, were the most widely used in paint. However, TBT found to be toxic to the most marine organisms, so led to regulations in many countries. The International Maritime Organization (IMO, 2001) banned on the TBT as an anti-fouling agent on ship from 1 January 2003 [4]. The alternative tin-free anti-fouling paints usually contain organic booster biocides. Primary organic booster biocides are shown in Table 1. and the biocides currently used are shown in Table 2. The fact that these chemicals are also toxic to aquatic life, therefore it is a need to develop a reliable analytical methodology to determine their concentrations in the marine environment. Several methods for analyzing Irgarol 1051 (Irgarol) was reported as follows: liquid–liquid extraction (LLE) or solid-phase extraction (SPE) followed by gas chromatography (GC) [5,6] or high-performance liquid chromatography (HPLC), and/or coupled to mass spectrometry (HPLC–MS) [7-13], coupled to diode array detector [14]. Irgarol 1051 is organic booster biocides that the use of these compound continues to

Table 1 Primary organic booster biocides (Source: [3])

Organic Booster Biocide	Trade Name
Heterocyclic Amines	
zinc complex of 2-mercaptopyridine-1-oxide	Zinc pyrithione
2-methylthio-4-butylamino-6-cyclopropylamine-s-triazine	Irgarol 1051
2,3,5,6-tetrachloro-4-(methylsulfonyl)pyridine	TCMSpryridine
(2-thiocyanomethylthio)benzothiazole	TCMTB
(4,5-dichloro-2-n-octyl-4-isothazolinj-3-one)	Sea-nine 211
pyridine triphenylborane complex	KH101
Aromatic Halides	
(2,4,5,6-tetrachloroisophthalonitrile)	Chlorothalonil
3-(3,4-dichlorophenyl)1,1-dinethylurea	Diuron
2,4,6-trichlorophenylmaleimide	
Carbamates	Ziram
zinc bis(dimethyl thiocarbamate)	Zineb
zinc ethylene bisdithiocarbamate bis(dimethylthiocarbamoyl)	Thiram
disulfide 3-iodo-2-propynyl butylcarbamate	Maneb
manganase ethylene bisdithiocarbamate	
Others	
N,N-dimethyl-N'-phenyl(N'-fluorodichloromethyl-thiosulfamide)	Dichlorofluanid
N-(fluorodichloromethylthio)phthalimide	
diiodomethyl-p-tolysulfone	

Table 2 Nomenclature and structures of organic booster biocides currently used in anti-fouling agents

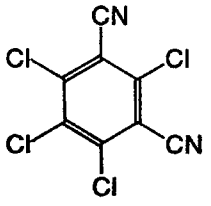

Chlorothalonil
(2,4,5,6-Tetrachloroisophthalonitrile)

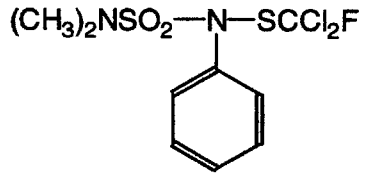

Dichlofluanid
(N-9-dimethyl-N-phenylsulphamid

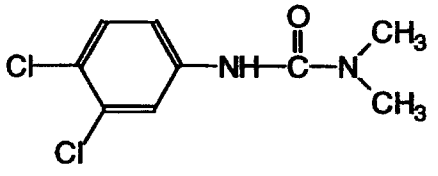

Diuron
(3-(3,4-dichlorophenyl)-1,1-dimethylurea)

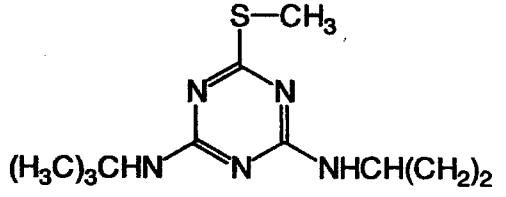

Irgarol 1051
(2-methylthio-4-tertiarybutylamino-6-cyclopropylamino-s-triazine)

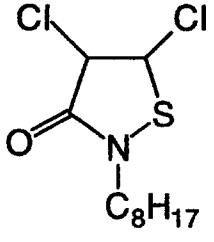

Sea-Nine 211
(4,5-dichloro-2-n-octyl-4-isothazolin-3-one)

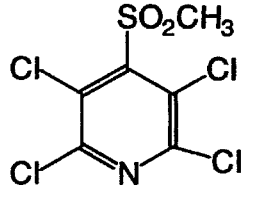

TCMS Pyridine
(2,3,5,6-tetrachloro-4-methylsulfonyl)pyridine

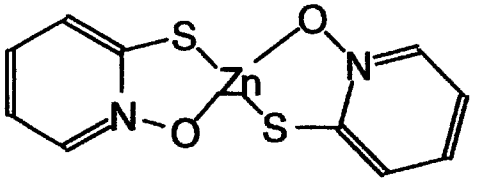

Zinc pyrithione
(bis(1-hydroxy-2(1H)-pyridethionato-o,s)-(T-4)zinc)

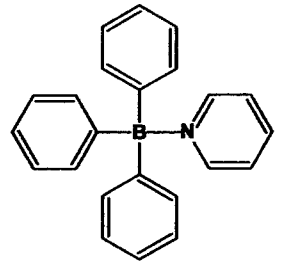

KH101
(Pyridine-triphenylborane, PTPB)

expand. In addition, Diuron [7-11, 14], Sea-Nine 211 [5, 6, 8, 10], chlorothalonil and dichlofluanid [5-8] was reported. However, chlorothalonil, Diuron and Irgarol 1051 were revoked because their high toxicity at low concentrations and their persistence in the environment [15].

Pyridine-triphenylborane (PTPB) is the most important booster biocide for tin-free anti-fouling agent in marine anti-fouling paint. PTPB is frequently used in some Asian countries because of its effectiveness [16]. PTPB was introduced commercially as an anti-fouling additive in Japan in 1993 [17] and used as a co-biocide by the formulation of a commercial paint containing it in Japan in 1995 [18]. PTPB is an excellent anti-fouling property with low water solubility, long lasting anti-fouling performance, and degrades rapidly after leaching into water [19]. Amey and Waldron proposed equations for the decomposition mechanism of PTPB in aqueous solution [19], the equations are shown in Figure 1. A few reports describe the analytical result of PTPB and also the degradation process of PTPB, its degradation products, and their toxicities to marine organisms [16, 19-24]. The degradation process of PTPB in water using HPLC-UV, have been reported [16, 19-22]. Okamura *et al.* [23] reported the risk of PTPB and its degradation products: DPB, MPB, phenol, and biphenyl, to two marine planktons. Thus, the toxicities, the 48 h LC50 values and the 72 h EC50 values for crustacean, *Artemia salina* and diatom, *Skeletonema costatum*, respectively, of the degradation products were not high compared to the PTPB. Kobayashi and Okamura [20] assessed the effects of eight biocides on sea urchin eggs and embryos. For these chemicals, toxicity appears to be in the order of zinc pyrithione > Sea-Nine 211 > pyridine-triphenylborane (KH101 or PTPB) > copper pyrithione > TBTO (tributyltin oxide) > Diuron - Irgarol 1051 > M1 (a degradation product of Irgarol 1051). In addition, Fukushi *et al.* [24] and auther *et al.* [25, 26]

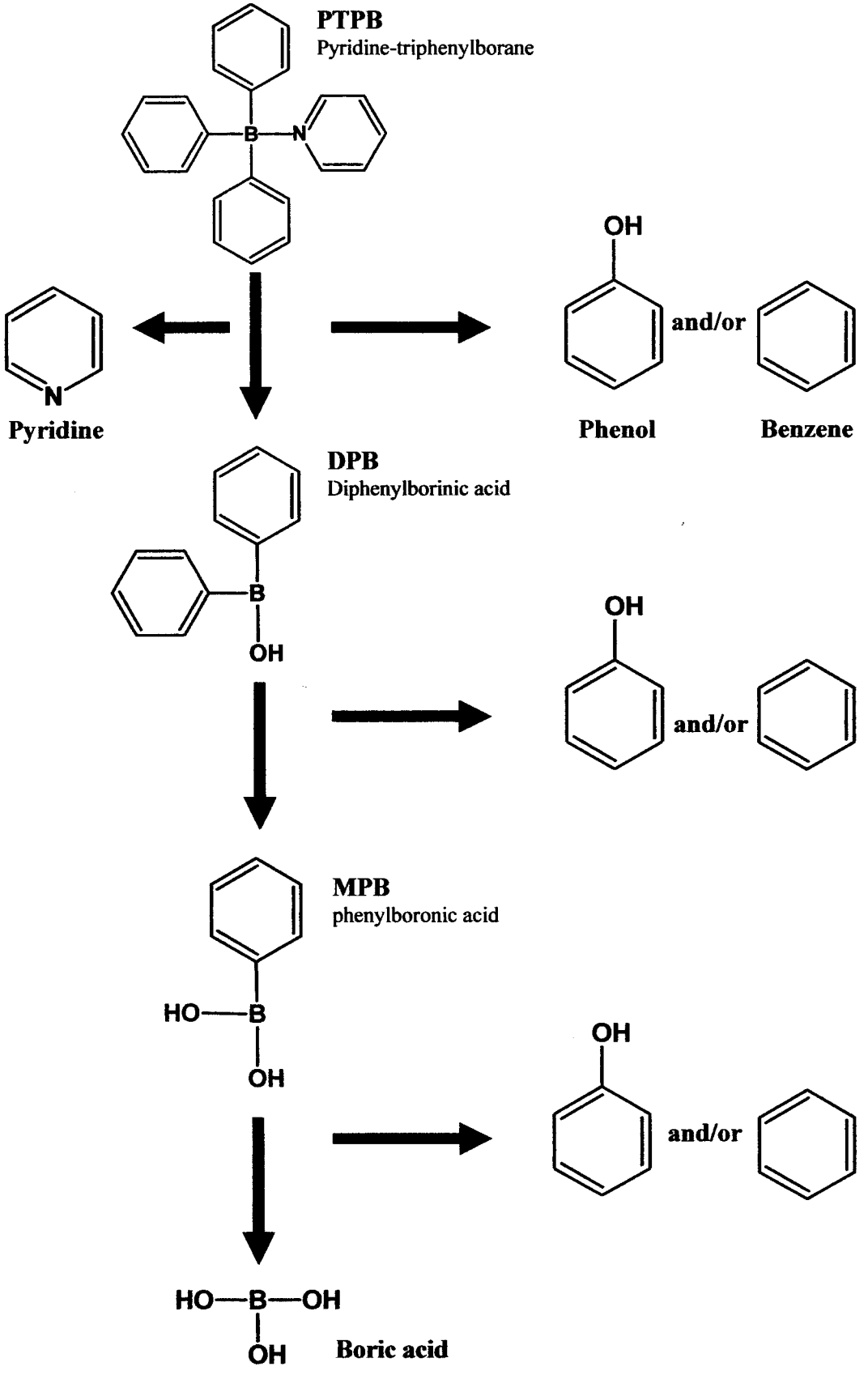

Figure 1. Decomposition of pyridine-triphenylborane

developed the capillary zone electrophoresis method for the determination of PTPB and its degradation products.

Capillary Zone Electrophoresis (CZE)

A Capillary Zone Electrophoresis (CZE) is now a mature technique for separation-based analysis that implies several advantages, such as high separation efficiency, minimum requirements for sample and reagents, and (much) more rapid analysis, over other separation techniques [27]. A CE instrument consists of an injection system, a separation capillary (20–200 mm I.D., 20–100 cm length), electrodes, a high voltage source (delivering up to 30 kV and up to 200–250 mA), and detector. Figure 2 illustrated a basic schematic of a CE instrument. In brief, the ends of a capillary are placed in a background electrolyte (BGE, separate buffer) reservoirs, each containing an electrode connected to a high-voltage power supply. The sample, containing a mixture of anions, cations, and neutral, is injected into the capillary by replacing one of the buffer reservoirs (normally at the anode) with a sample reservoir and applying either an electric potential or external pressure for a few seconds. After replacing the buffer reservoir, an electric potential is applied across the capillary and the separation is performed. The separated analytes toward to the detector (normally UV-vis) near the opposite end (normally at the cathode) can be achieved detection directly through the capillary wall. The basic concept of the separation process in Capillary Zone Electrophoresis (CZE) is based on the difference in the migration velocity (speed of migration) of ions or neutrals under the influence of an electric field. The mechanisms separation of CZE as follows. The silanol groups in uncoated silica capillaries, is typically used for CE, which are in

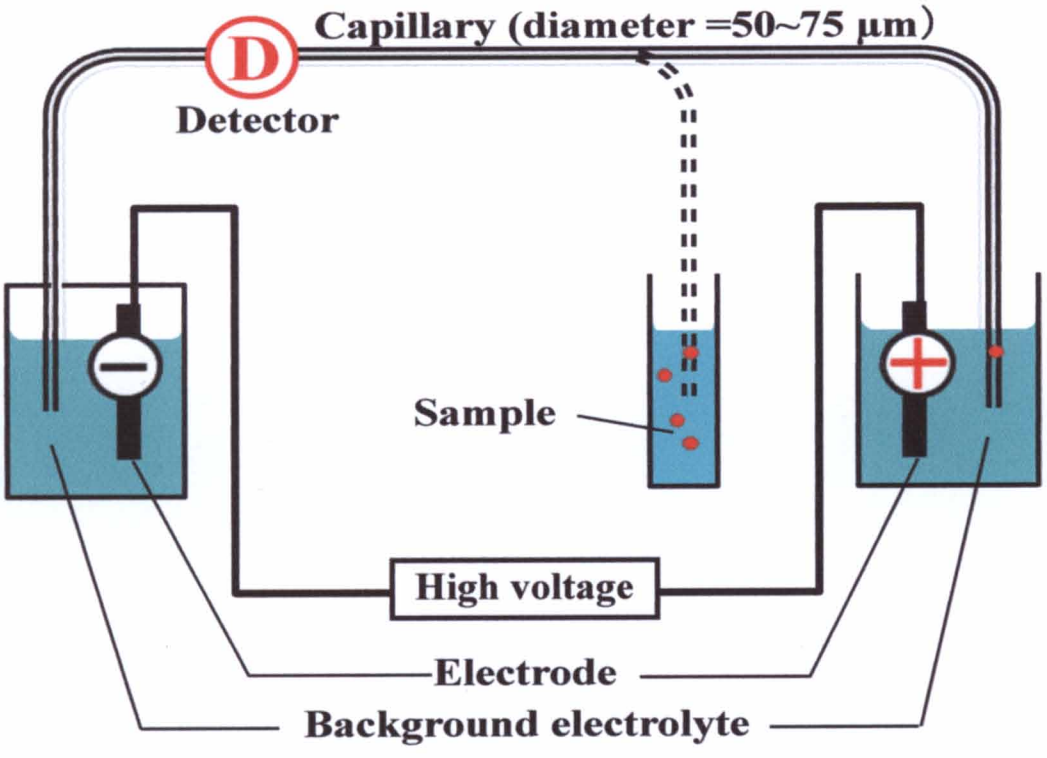

Figure 2. Basic schematic of a CZE instrument

contact with the buffer. These silanol groups readily dissociate, giving the capillary wall a negative charge. Therefore, when the capillary is filled with buffer, the positive charged of the buffer are attracted to the negative charges of the capillary wall forming an electrical double layer. When applying voltage, the mobile cation in the double layer flow toward the cathode, creating a bulk flow of the buffer in that direction. This flow is called electroosmotic flow (EOF) depicted in Figure 3(A). The electroosmotic flow drives all ions and neutrals in the capillary towards the cathode which is generally in the direction of the detector. Difference ions and neutrals will move at different migration velocity depending on their electrophoretic mobilities at the same electric field strength.

The electrophoretic migration velocity (v) of ion (migration velocity of each ion) depends on its electrophoretic mobility (μ_{ep}), and on the applied electric field (E) and is described by the following equation:

$$v = \mu_{ep}E \qquad (1)$$

Where v = electrophoretic migration velocity (m s^{-1}); μ_{ep} = electrophoretic mobility (m^2 V^{-1} s^{-1}); E = electric field strength (V m^{-1}).

The electric field strength (E) is described by the following equation:

$$E = V/L \qquad (2)$$

Where V = potential (V); and L = capillary length (cm).

Electrophoretic mobility (μ_{ep}) is a factor that indicates how fast an ion or neutral move through a buffer solution. Which μ_{ep} is described by the following equation

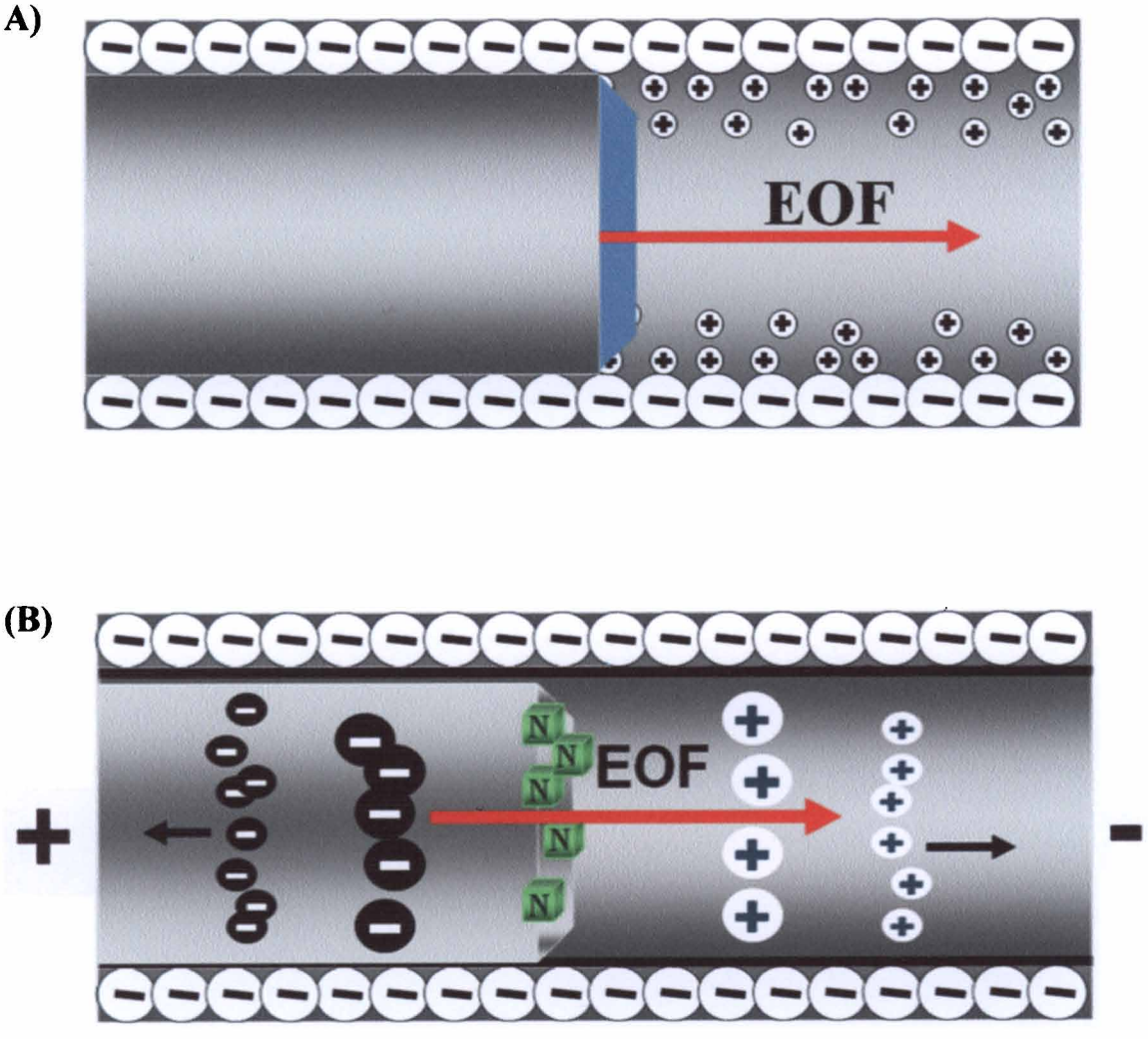

Figure 3. (A) Electroosmotic flow (EOF); (B) Electrophoretic mobility

$$\mu_{ep} = \frac{q}{6\pi\eta r} \qquad (3)$$

Where q = ion charge; r = ion radius; η solution viscosity.

From equation (3) can see that difference in electrophoretic mobility will be caused by differences in the charge-to-size ratio of analyte ions. Higher charge and smaller size confer greater mobility, whereas lower charge and larger size confer lower mobility.

Electrophoretic mobility is the important concept to understand in electrophoresis. This is because electrophoretic mobility is a characteristic property for each ion or neutral and will always be a constant. The different ions and neutrals have different electrophoretic mobilities, so they also have different migration velocities at the same electric field strength. It is possible to separate mixtures of different ions and solutes by using electrophoresis.

The sample consists of cationic analyte, an anionic analyte, and neutral solute, which all analytes moves to the cathode with the velocity of the electroosmotic flow (v_{eo}). The linear velocity of the EOF (υ_{eo}) is described by the following equation:

$$\upsilon_{eo} = \left(\frac{\varepsilon\zeta}{4\pi\eta}\right) E \qquad (4)$$

Where ε = the dielectric constant of the buffer; ζ = the zeta potential; η = the viscosity of the buffer; E = the applied electric field. The terms enclosed in brackets equate to the mobility of the EOF (μ_{eo}).

$$\mu_{eo} = \frac{\upsilon_{eo}}{E} \qquad (5)$$

Mobility of EOF (μ_{eo}) (electroosmotic mobility) is greater than that of most analysts, it follows that cations, neutral species then anions, in this sequence, will pass through the detector in the same run. The time required for each species to migrate to the detector, so called migration time.

The electrophoretic mobility (μ_{ep}) of each analyte can be calculated from an electropherogram. A apparent's analyte electrophoretic mobility (μ_a), that is calculated from its apparent migration velocity, is the vector sum of its real (or effective) electrophoretic mobility (μ_{ep}) and the EOF mobility (μ_{eo})

$$\mu_a = \mu_{ep} + \mu_{eo} \qquad (6)$$

$$\mu_{ep,i} = \frac{v_{ep}}{E} = \frac{L_D \cdot L_T}{t_i V} \qquad (7)$$

$$\mu_{eo} = \frac{\overline{v_{eo}}}{E} = \frac{L_D \cdot L_T}{t_{eo} V} \qquad (8)$$

Where L_D = effective capillary length (cm); L_T = total capillary length (cm); t_i = migrationtime of analyte i (s); t_{eo} = migration time of the EOF marker (s); V = potential (V).

Since samples are normally introduced at the anode and EOF moves from the anode to the cathode, cations have positive μ_{ep}, neutrals have zero μ_{ep} and, anions have negative μ_{ep}. In other words, cations migrate faster than the EOF and anions migrate more slowly than the EOF. Neutrals migrate with the same velocity as the EOF.

A feature of EOF in CZE has a flat flow profile because its driving force, charge on

the capillary wall, is uniformly distributed along the capillary and the flow velocity is uniform across the capillary. This contrasts with pressure-driven flow, such as in HPLC, in which frictional forces at the column walls cause a pressure drop across the column. The flat profile of EOF is important because it minimizes zone broadening during the electrophoretic migration, leading to high separation efficiencies

Two modes of conventional sample injection modes currently used in CE, hydrodynamic and electrokinetic mode. The former, is more widely used, the precisely estimated volume of sample injected can be obtained. Sample introduced into the capillary using pressure or vacuum application while the injection end of the capillary is dipped in the sample solution, is non-selective, any analytes including neutral are injected have the same composition as the sample solution. While the latter, induced by application of potential, is selective (the ions in the sample are injected depends on the mobility and charge).

Hydrodynamic injection mode, the amount of samples can be introduced into the capillary is described by the Poiseuille law:

$$\text{Amount} = \frac{\Delta P r^4 \pi C t}{8 \eta L} \qquad (9)$$

Where ΔP = pressure difference; r = inner radius; C = sample concentration; t = injection time; η = solution viscosity; L = capillary length.

From the above equation, the amount of analytes injected depending on sample concentration, pressure and, injection time.

In the electrokinetic injection mode, the sample loaded is described by the equation

below:

$$\text{Amount} = \frac{(\mu_{ep} + \mu_{eo})\ \pi r^2 C t}{L} C \qquad (10)$$

Where: μ_{ep} = electrophoretic mobility of analyte; μ_{eo} = electroosmotic flow (EOF) mobility; r = inner radius; V = potential; C = sample concentration; t = injection time; L = capillary length.

From the above equation, the amount of analytes injected by electrokinetic injection depends on the EOF and the electrophoretic mobility of the analyte. The electrokinetic injection is the possible selective injection technique because only charged analytes can be successfully injected. Comparison of electrokinetic and hydrodynamic injection is shown in Table 3.

The detection in CE, UV absorption detection is almost universally adopted in CE. In fact, all commercial CE instruments available today employ UV-VIS absorbance detectors. UV detection mostly applied in the on-column mode with a modified optical layout through a window obtained by burning off the polyimide coating on the outside of the capillary. The high transparency of the fused-silica capillary wall allows the use of low UV wavelengths (down to 190 nm). On the other hand, the path length is very short which is the limits of the capillary diameter (20–100 μm), and according to the Beer's law ($A = \varepsilon bC$, where A = absorbance; ε = molar absorptivity; b = optical path length; C = concentration) the detection limits is lower than 10^{-6} M [29]. In addition to UV absorotion several other detection techniques have successfully been adopted in CE, with advantages in sensitivity and/or selectivity, such as fluorescence detection, conductimetric detection, and mass spectrometric (MS) detection.

Table 3 Comparison of electrokinetic and hydrodynamic injections [28]

Parameter	Electrokinetic injections	Hydrodynamic injections
Selectivity of injection	Selective for ions	Non-selective
Repeatability	0.2 – 2% for migration time 2 – 5% for peak area	0.1 – 0.5% for migration time 0.5 – 3% for peak area
Dynamic range	1 – 2 orders of magnitude	2 – 3 orders of magnitude
Sensitivity	Relatively high, but ion-dependent	Relatively low
Matrix effect	Significant	Negligible
Main application area(s)	Sample preconcentration	Routine quantitative analysis

As above mentioned, A UV-VIS absorbance detector is generally used in CE. However, the concentration sensitivity CE-UV is fairly poor because a small inner diameter of the capillary limits the optical path length for detection. Therefore, the development the CZE method with UV detection to enhance the sensitivity is the purpose of this study for simultaneous determination of PTPB and its degradation products: DPB, MPB, and phenol.

This thesis consists of three chapters. In Chapter one, field-amplified sample injection (FASI) procedure developed and applied to the determination of PTPB, DPB, MPB, and phenol in paint wastes obtained from shipyards around Osaka Bay. In Chapter two, a novel sample injection method given name hybrid sample injection mode (HSIM) was proposed. HSIM was the combination of FASI and vacuum injection proposed to enhance the detection sensitivity. The HSIM procedure is simple and useful for enhancing the sensitivity. In Chapter three, a CZE method developed for the simultaneous determination of PTPB, DPB, MPB, and phenol in artificial seawater (ASW) without any extraction procedure. The developed CZE method is a simple procedure and no need of complicated and costly for the sample pretreatment procedure that is to be useful for the determination of the degradation process of PTPB and its degradation products in ASW.

Reference

1. Peñalver, E., Borrull, F., Marcé, R. M., *J. Chromatogr. A* 1999, *839*, 253-260.
2. Dafforn, K. A., Lewis, J. A., Johnston, E. L., *Mar. Pollut. Bull.* 2011, *62*, 453-465.
3. Omae, I., *Appl. Organometal. Chem.* 2003, *17*, 81-105.
4. IMO, *International Maritime Organisation*, 2001, London.

5. Agüera, A., Piedra, L., Hernando, M. D., Ferández-Alba, A. R., *J. Chromatogr. A* 2000, *889*, 261-269.

6. Hernando, M. D., Piedra, L., Belmonte, A., Agüera, A., *J. Chromatogr. A* 2000, *889*, 261-269.

7. Ferrer, I., Barceló, D., *J. Chromatogr. A* 1999, *854*, 197-206.

8. Martinez, K., Ferrer, I., Barceló, D., *J. Chromatogr. A* 2000, *879*, 27-37.

9. Okamura, H., *Chemosphere* 2002, *48*, 43-50.

10. Okamura, H., Watanabe, T., Aoyama, I., Hasobe, M. *Chemosphere* 2002, *46*, 945-951.

11. Gimeno, R. A., Aguilar, C., Marcé, R. M., Burrull, F., *J. Chromatogr. A* 2001, *915*, 139-147.

12. Lam, K.-H., Lei, N.-Y., Tsang, V. W.-H., Cai, Z., Leung, K. M. Y., *Mar. Pollut. Bull.* 2009, *58*, 272-279.

13. Cai, Z., Fun, Y., Ma, W.-T., Lam, M. H.-W., Tsui, J., *Talanta* 2006, *70*, 91-96.

14. Gatidou, G., Kotrikla, A., Thomaidis, N. S., Lekkas, T. D., *Anal. Chim. Acta.* 2005, *528*, 89-99.

15. Cresswell, T., Richards, J. P., Glegg, G. A., Readman, J.W., *Mar. Pollut. Bull.* 2006, *52*, 1169-1175.

16. Okamura, H., Kitano, S., Harino, H., Thomas, K. V., *Chemosphere* 2009, *74*, 1275-1278.

17. *Japan Chemical Daily,* 1993, June 25, 3.

18. Chugoku Marine Paints, Inc., Private Communication, 2002.

19. Amey, R., Waldron, C., *in Proceedings of International Symposium on Antifouling Paint and Marine Environment.*, Tokyo, 2004, 234-243.

20. Kobayashi, N., Okamura, H., *Mar. Pollut. Bull.* 2002, *44*, 748-751.

21. Harino, H., *Coastal Mar Sci.* 2004, *29(1)*, 28-39.

22. Takahashi, K., Yoshikawa, E., Akiyama, M., Kitaori, K., Masuoka, S., *J. Jpn. Colour Mater.* 2005, *78(2)*, 50-57.

23. Zhou, X., Okamura, H., Nagata, S., *Chemosphere* 2007, *67*, 1904-1910.

24. Fukushi, K., Yakushiji, Y., Okamura, H., Hashimoto, Y., Saito, K., *J. Chromatogr. A* 2010, *1217*, 2187-2190.

25. Kaewchuay, N., Yakushiji, Y., Fukushi, K., Saito, K., Hirokawa, T., *Electrophoresis* 2011, *32*, 1486-1491.

26. Kaewchuay, N., Fukushi, K., Tsuboi, A., Okamura, H., Saito, K., Hirokawa, T., *Anal Sci.*2012, *28*, 1191-1196.

27. Zheng, L., Zhang, L., Tong, P., Zheng, X., Chi, Y., Chen, G., *Talanta* 2010, *81*, 1288-1294.

28. Krivácsy, Z., Gelencsér, A., Hlavay, J., Kiss, G., Sárvári, Z., *J. Chromatogr. A* 1999, *834*, 21-44..

29. Kuhn, R., Hoffstetter-Kuhn, S., *Capillary Electrophoresis Principle and Practice, Springer-Verlag*, Berlin, 1993.

Chapter 1

Simultaneous Determination of Pyridine-Triphenylborane Anti-Fouling Agent and Its Degradation Products in Paint-Waste Samples Using Capillary Zone Electrophoresis with Field-Amplified Sample Injection

1. Introduction

Over the past decades of successful development, capillary electrophoresis (CE) has matured as an established separation technique in several application areas with recognized advantages of simplicity, separation efficiency, minor sample ans solvent consumption. However, CE has a low concentration sensitivity from minute sample volumes (at the nL level), and a short optical path length (typically 25 – 100 μm) available with UV detection [1]. Different types of in-line sample concentration techniques have been proposed to enhance the CE sensitivity: large volume sample stacking [2], large-volume sample stacking with an electroosmotic flow (EOF) pump (LVSEP) [3, 4], sweeping [5-7], dynamic pH junction [8, 9], field-amplified sample injection (FASI) [10-15], two-end field amplified sample injection (TE-FASI) [16], acetonitrile (ACN)-mediated stacking [17], isotachophoresis (ITP) and transient ITP [18-20], electrokinetic supercharging (EKS) [21-23], counter-flow electrokinetic supercharging (CF-EKS) [24], pressure-assisted injection techniques [25, 26], and simultaneous electrokinetic and hydrodynamic injection (SEHI) [27, 28]. These procedures are useful, but some were somewhat complicated in their application to real

samples. FASI is a popular and simple online enrichment technique by which samples are prepared in a highly diluted background electrolyte (BGE) or water. A sample is introduced into the capillary using hydrodynamic or electrokinetic injection (EKI). Furthermore, the injection of a short plug of water into the column before sample introduction with EKI was proposed to insure proper field amplification (FASI with water plug) [10]. This procedure is expressed hereinafter as just FASI. Analytes are stacked at the interface between the water plug and the BGE because of the higher electric field strength in the water plug than that in the BGE. Similar procedures were also developed using a plug of organic solvent, such as methanol, ACN, and their mixture instead of the water plug [13].

An anti-fouling agent, pyridine-triphenylborane (PTPB), is usually applied to ship hulls to prevent unnecessary fuel consumption resulting from the buildup of marine organisms, such as barnacles and bivalves. Over time, they adhere to ship hulls surfaces. However, anti-fouling agents are harmful to non-target marine organisms [29]. The characteristics of an ideal anti-fouling agent are that it be long-lasting, but easily degradable to less toxic compounds for marine organisms shortly after dissolving in seawater. Developing an analytical method for these compounds is important to elucidate their degradation products and their toxicities to marine organisms. Reportedly, PTPB can degrade to diphenylborinic acid (DPB), phenylboronic acid (MPB), phenol, and other materials. Conventionally, HPLC has been used for the determination of PTPB [30-32]. According to a procedure described by Takahashi *et al.* [32], the four analytes listed above are detectable, but DPB and MPB were not separable [29]. Although PTPB and DPB were simultaneously detectable using HPLC, another analytical condition, including the use of a different column had to be used for the simultaneous determination

of MPB and phenol [33]. Consequently, no analytical method is available for the simultaneous determination of PTPB, DPB, MPB, and phenol, except for our previous methods [34, 35].

We previously developed a capillary zone electrophoresis (CZE) with direct UV detection for the simultaneous determination of PTPB, DPB, MPB, and phenol [34]. Furthermore, a novel hybrid sample injection mode (HSIM) that presents the combination of FASI and vacuum injection was proposed to enhance the detection sensitivity [35]. In fact, HSIM cannot be used for some commercial instruments: EKI and vacuum injection modes are inapplicable simultaneous. Moreover, when the HSIM is applied to the analysis of real samples, such as paint wastes, its separation efficiency might be degraded because of coexisting substances in the samples and the sample solvent introduced simultaneously. Presumably, FASI is advantageous compared to HSIM from the standpoint of its extensive utility and separation efficiency for real samples. Therefore, this study used FASI for applications to real samples. The analytical conditions, time of water plug injection, time, and voltage of sample introduction were examined and optimized. Boer and Ensing [36], and Hirokawa *et al.* [37, 38] reported that the efficiency of EKI and EKS is strongly related to the electrode configurations. Therefore, we investigated the effects of the distance between the tip of the electrode and a capillary end (D_{ec}) on the peak heights for the analytes listed above using FASI. Biocide-based anti-fouling paints are an important localized source of trace elements (particularly copper and zinc) and organic biocide in water [39]. The procedure established in this study was therefore applied to the determination of PTPB, DPB, MPB, and phenol in paint wastes obtained from shipyards around Osaka Bay in Japan. This is the first reported attempt to use FASI-CZE as a simple and sensitive procedure for the

analysis of PTPB and its degradation products in real samples, such as paint wastes.

2. Experiments

2.1. Apparatus

The CE apparatus used throughout this study was equipped with a UV-vis absorbance detector (270A-HT; Perkin-Elmer, Foster City, CA). The rise time for the detector was set at 0.5 s. A polyimide-coated fused-silica capillary was used (75 μm i.d. × 375 μm o.d.; GL Sciences, Tokyo, Japan). The total length of the capillary was 72 cm; its effective length was 50 cm. The peak area, peak height, and migration time were measured using a Chromato-Integrator (D-2500; Hitachi, Tokyo, Japan). The pH measurements were carried out using a pH meter (F-22; Horiba, Kyoto, Japan). PTPB and its degradation products were extracted from paint-waste samples using a shaker (RECIPRO SHAKER SR-25; Taitec, Saitama, Japan), a centrifuge (KUBOTA 3700; Kubota Seisakusho, Tokyo, Japan), and a rotary evaporator (RE300; Yamato Kagaku, Tokyo, Japan).

2.2. Reagents

All reagents were of analytical-reagent grade and used as received. PTPB, DPB, and MPB were obtained from Hokko Chemical (Tokyo, Japan). Phenol was the product of Nacalai Tesque (Kyoto, Japan). Individual stock solutions (1000 mg L^{-1}) of PTPB, DPB, MPB and phenol were prepared in ACN purchased from Nacalai Tesque. To keep the stability of the stock solutions for a long time, 1% (v/v) pyridine (Nacalai Tesque) was

added (except for phenol), and the solutions were then covered with an aluminum foil and kept at 4°C to prevent their degradation. Standard solutions used for the examination of analytical conditions and building-up the calibration graphs were prepared by serial dilutions of the stock solutions with ACN. Hexane, dichloromethane, ethyl acetate, and methanol obtained from Wako Pure Chemical Industries (Osaka, Japan) were used as extracting reagents for paint-waste samples. The extracted solutions were passed through a silica-gel column (MEGA BE-SI: 1 g, 6 mL; Varian Inc., Palo Alto, CA) for clean-up and preconcentration. The pH of the BGE (a 20-mM solution of sodium tetraborate) was adjusted to 9.8 using 1 M NaOH (Nacalai Tesque). The BGE was filtered through a 0.45-μm membrane filter (Advantec Toyo Kaisha, Tokyo, Japan) before use. Distilled, deionized water, obtained from an automatic still (WG220; Yamato Kagaku) and a Simpli Lab-UV high-purity water apparatus (Merck Millipore, Tokyo, Japan) were used throughout.

2.3. Sample preparation

Three paint-waste samples were obtained from shipyards along the coast of the Osaka Bay, located in Osaka city (wastes I and II) and in Aioi city (waste III) in Japan. When ship hulls were sandblasted with high pressure in docks, some fragments came off. They were collected, and served as the samples after drying. The ingredients of these samples could be dissolved into the sea when ships were on a voyage, at anchor, or in port. PTPB and its degradation products were extracted from the paint-waste samples according to the following procedure [40]. The sample (2.5 g) in 25 mL of dichloromethane was shaken at 200 rpm for 6 h. The resultant solution was centrifuged at

2000*g* for 10 min. The supernatant solution in an eggplant-shape flask was evaporated to dryness *in vacuo* below 40°C. The residue in the eggplant-shape flask was dissolved with 5 mL of hexane, and the solution was passed through the silica-gel column precleaned using 5 mL of methanol, ethyl acetate, dichloromethane, and hexane. Then, 5 mL of dichloromethane, ethyl acetate, and methanol were separately added to the eggplant-shape flask in this order. Each solution was passed through the column successively to elute the analytes. Each eluate was dried up by blowing a nitrogen stream. The residue was dissolved with 2 mL of ACN containing 1% (v/v) pyridine. From preliminary experiments, it was found that all analytes were detected in the ethyl acetate fractions. Phenol was detected in both the dichloromethane and methanol fractions, but the concentrations were less than the ethyl acetate fractions. In this study, the ethyl acetate fractions were analyzed to evaluate the applicability of the proposed method to paint-waste samples. The resultant solutions of the ethyl acetate fractions were diluted 50 times for waste I, 20 times for waste II, and 300 times for waste III with ACN to avoid interference from coexisting anions derived from substances present in the paint wastes. The diluted samples and those added with 5 – 200 μg L^{-1} of PTPB, DPB, MPB, and phenol, were analyzed using the method. The concentrations of these compounds in the paint wastes were calculated using the standard addition procedure and calibration graphs.

2.4. CZE procedure

New capillaries were pretreated by flushing with 1 M NaOH for 40 min and then with water for 10 min. The following optimum analytical conditions were established.

Before the first analysis of each day, the capillary was washed with water for 5 min, 1 M NaOH for 5 min, and water for 10 min. The capillary was thermostated at 30°C. The detection wavelength was set at 200 nm as the signal-to noise ratios for all compounds had maximum values [34]. A BGE, 20 mM sodium tetraborate was adjusted to pH 9.8 with 1 M NaOH. Between runs, the capillary was flushed with 0.1 M NaOH for 3 min. It was then filled with the BGE for 3 min. Subsequently, water was injected by the application of a vacuum (16.9 kPa) for 2 s (corresponding to 42 nL), and the sample solution was injected into the capillary using FASI (5 kV for 6 s, at the sample inlet side as the cathode). The vertical distance between the tip of the electrode and the capillary end (D_{ec}) was set at 0.5 mm as a default D_{ec}. The electrode tip was kept higher than the capillary end. Each step was run automatically. After each analysis, a constant volume of the sample (600 μL) was newly filled in the vial. The BGEs of the sample inlet side and the detector side were renewed for every two and four injections, respectively. The capillary was flushed with water for 5 min to fill the capillary with water at the end of the day. Calibration graphs were prepared using synthetic standards.

3. Results and discussion

3.1. Strategy for separation and sensitivity enhancement

We adopted the FASI procedure to separate and to enrich the low concentrations of analytes in paint waste samples because of its higher separation efficiency and simplicity, as described in the Introduction. The same BGE, adjusted to pH 9.8, as used in our previous study [35], was adopted here so that the all analytes would exist as anions in the alkaline BGE. The sample inlet side must be set as the cathode to inject the analytes into

the capillary using FASI. However, the EOF works to push the analytes back to the sample vial. That is to say, the amount of injected analytes depends on the difference between the magnitude of electrophoretic migration of the analytes and that of EOF: higher mobility of analytes can be introduced more than lower mobility of analytes in the same magnitude of EOF. Therefore, the applied voltage and the time for sample introduction must be optimized. It is also important to ascertain the optimum injection time for a water plug, since the sensitivity and reproducibility were reportedly improved by injecting the water plug into the capillary [10].

Hirokawa *et al.* [37] described the effectiveness of prolonging the vertical distance between the tip of the electrode and the capillary end (D_{ec}) to obtain high sensitivity in EKS-CZE. The amount of sample injected into the capillary can be increased by extending D_{ec}. It might be worthwhile to use long D_{ec} in this study. Dawod *et al.* [24] used a hydrodynamic counter-flow to minimize the introduction of the sample matrix into the capillary, thus allowing longer injections to be performed in EKS-CZE. The direction of the counter-flow was from the outlet to the inlet vials to balance the reversed EOF while applying the negative potential to inject the sample into the capillary. Meighan *et al.* [26] similarly applied positive pressure to allow long EKI to be performed. A negative potential was applied to inject the sample into the capillary with a positive pressure towards the anode (the outlet vial) to balance the EOF. These are attractive procedures to determine low concentrations of analytes. However, the hydrodynamic counter-flow proposed in the former procedure was inapplicable in the CE apparatus used in the present study. The latter procedure was apparently similar to the HSIM proposed previously [35].

3.2. Effect of water plug

A mixture of 0.5 mg L^{-1} PTPB, DPB, MPB, and phenol was analyzed using FASI (sample injection, 5 kV for 6 s) with default D_{ec} (0.5 mm). The vacuum injection time for the water plug was varied between 0.5 and 3 s. The results are depicted in Figure 1. The peak height for PTPB increased with the injection time up to 1 s, leveled off to 1.5 s, and then decreased. The peak height for DPB increased to 1 s, leveled off to 2 s, and then decreased. The peak heights for MPB and phenol increased when going to 2 s and then decreased slightly. The tendency presented above is explainable as follows. The water plug provided a higher electric field because of its lower conductivity, which facilitated sample stacking. However, a further increase of the water plug would cause diffusion of the analyte zones [132]. The optimum injection time of the water plug depends on the analyte. For 2 s, the maximum peak heights were obtained for DPB, MPB, and phenol, except for PTPB. When the injection time was 2 s, the RSDs of peak heights for PTPB, DPB, MPB, and phenol (2.6 – 16%) were smaller than those for 0.5 s (11 – 24%) and 1 s (12 – 19%) and similar to those for 1.5 s (7.4 – 18%), 2.5 s (2.9 – 18%), and 3 s (5.9 – 15%). Therefore, the optimum injection time of the water plug adopted in the subsequent experiments was 2 s.

3.3. Effect of sample-injection voltage

The sample-injection voltage was varied between 3 and 7 kV using FASI with the sample injection time for 6 s. The same sample as that described in the former section was used. As apparent in Figure 2, the peak heights for PTPB, DPB, MPB, and phenol

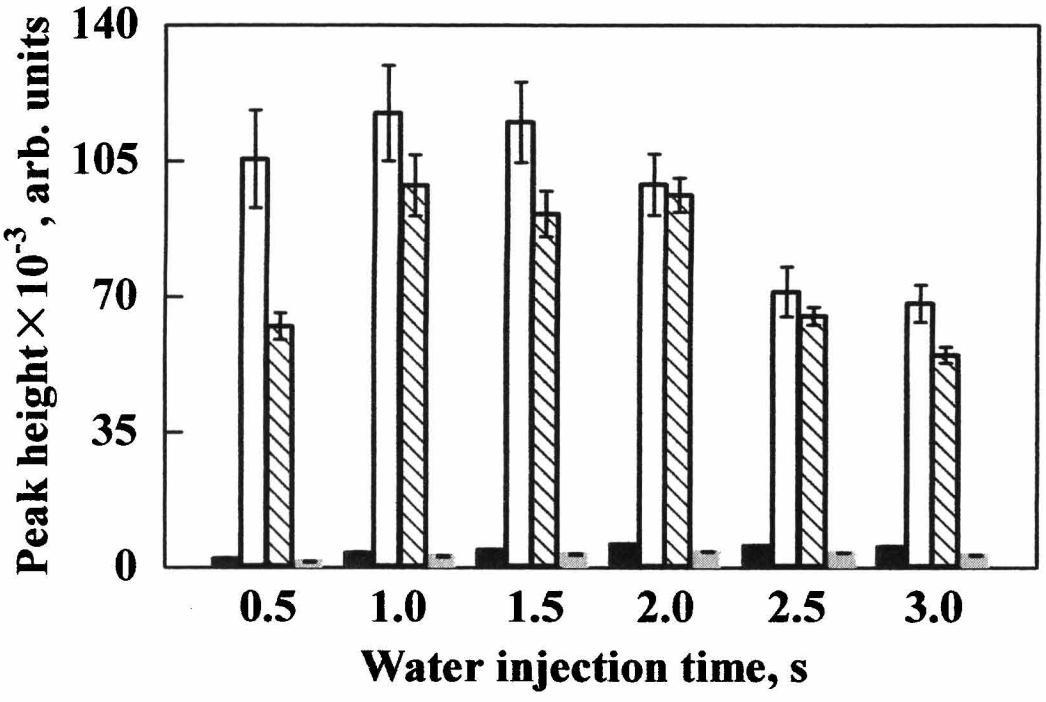

Figure 1. Effect of injection time of water plug on the peak height. Each bar corresponds to phenol, PTPB, DPB, and MPB, respectively, from left to right. Sample injection: 5 kV for 6 s. CZE conditions: capillary, 50/72 cm × 75 μm id; BGE, 20 mM sodium tetraborate adjusted to pH 9.8 with 1 M NaOH; voltage, 15 kV; wavelength for detection, 200 nm. Sample, 0.5 mg L^{-1} of each analyte in ACN.

increased concomitantly with increasing injection voltage up to 5 kV, and then decreased. The maximum peak heights were obtained for all analytes when the voltage was set at 5 kV. The RSDs of the peak heights for all analytes (2.6 – 18%) were almost identical for the injection voltages. Therefore, 5 kV was used further as the optimum injection voltage.

3.4. Effect of sample-injection time

The sample-injection time was varied between 4 and 8 s, with the injection voltage set at 5 kV using the same sample as in the former section. The results are portrayed in Figure 3. The peak height for PTPB increased with the injection time up to 7 s, and then decreased. The peak heights for DPB, MPB, and phenol increased concomitantly with increasing injection time up to 6 s, and then decreased. The maximum peak heights were obtained for DPB, MPB, and phenol, except for PTPB when the sample-injection time was 6 s. The RSDs of peak heights for all analytes (2.6 – 19%) were almost identical among the injection times. Therefore, 6 s was chosen as the optimum sample injection time.

A mixture of PTPB, DPB, MPB, and phenol was analyzed using FASI under the optimum conditions (injection time of the water plug, 2 s; sample injection, 5 kV for 6 s) to compare the results obtained using EKI (5 kV for 6 s). The peak heights for PTPB and DPB using the FASI (Figure 4(A)) were, respectively, 16 and 58 times higher than those obtained using the EKI. The chemical form of PTPB detected was supposed to be triphenylborane because of the migration order of the four compounds and the description in the reference [29].

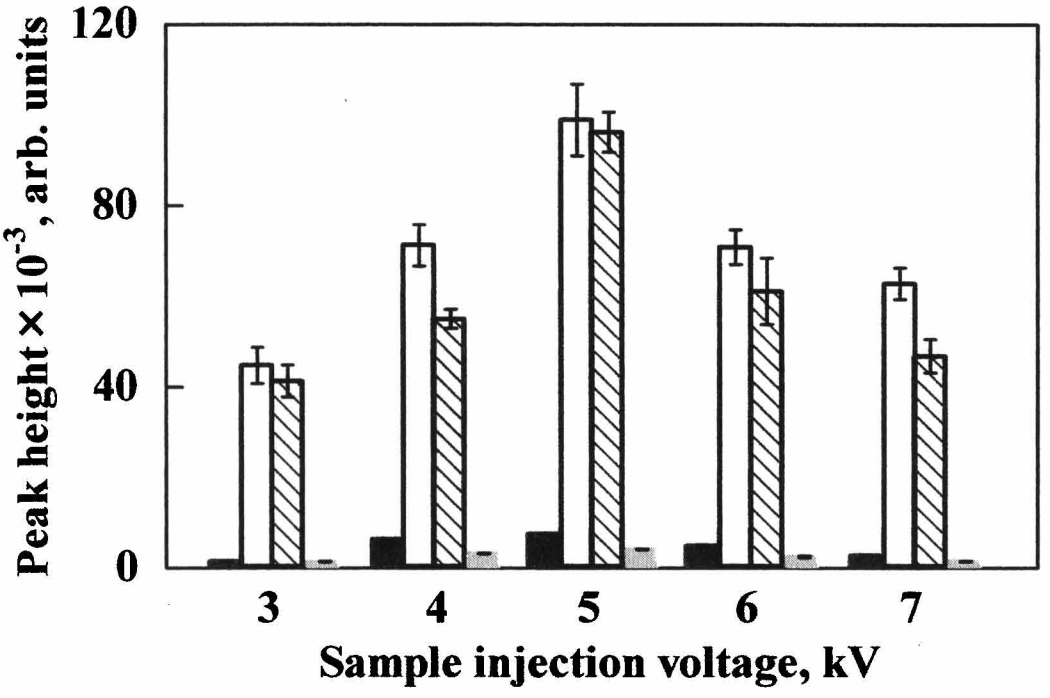

Figure 2. Effect of sample injection voltage on the peak height. Water plug was vacuum injected for 2 s (42 nL) prior to sample introduction. Each bar corresponds to phenol, PTPB, DPB, and MPB, respectively, from left to right. Sample, 0.5 mg L^{-1} of each analyte in ACN. CZE conditions are as in Figure 1.

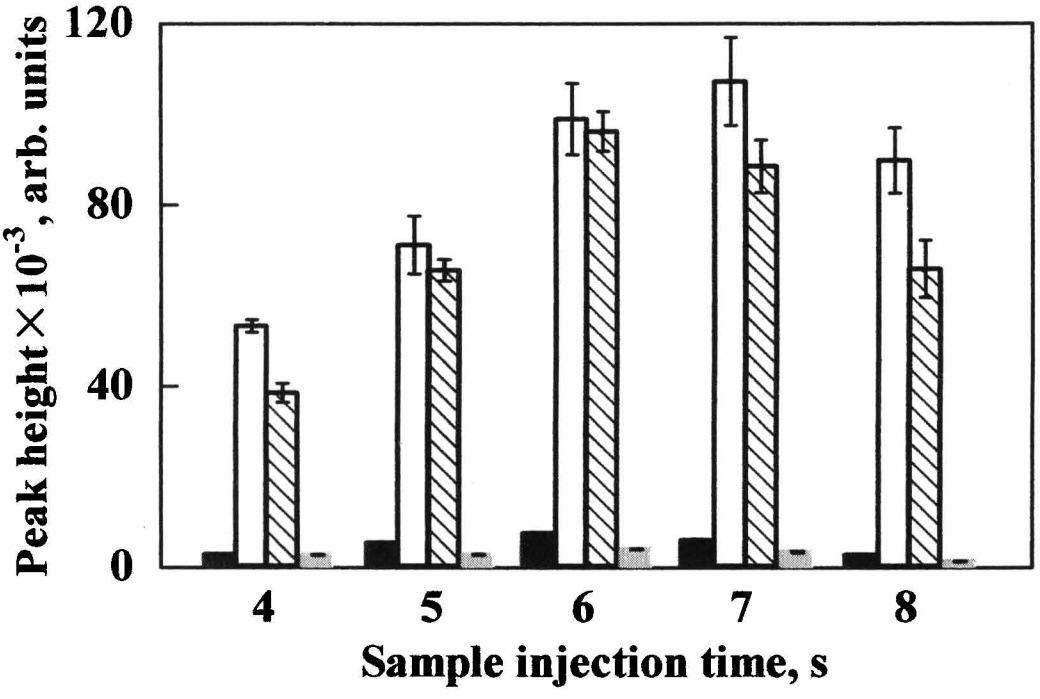

Figure 3. Effect of sample injection time on the peak height. Water plug was vacuum injected for 2 s (42 nL) prior to sample introduction. Each bar corresponds to phenol, PTPB, DPB, and MPB, respectively, from left to right. Sample, 0.5 mg L^{-1} of each analyte in ACN. CZE conditions are as in Figure 1.

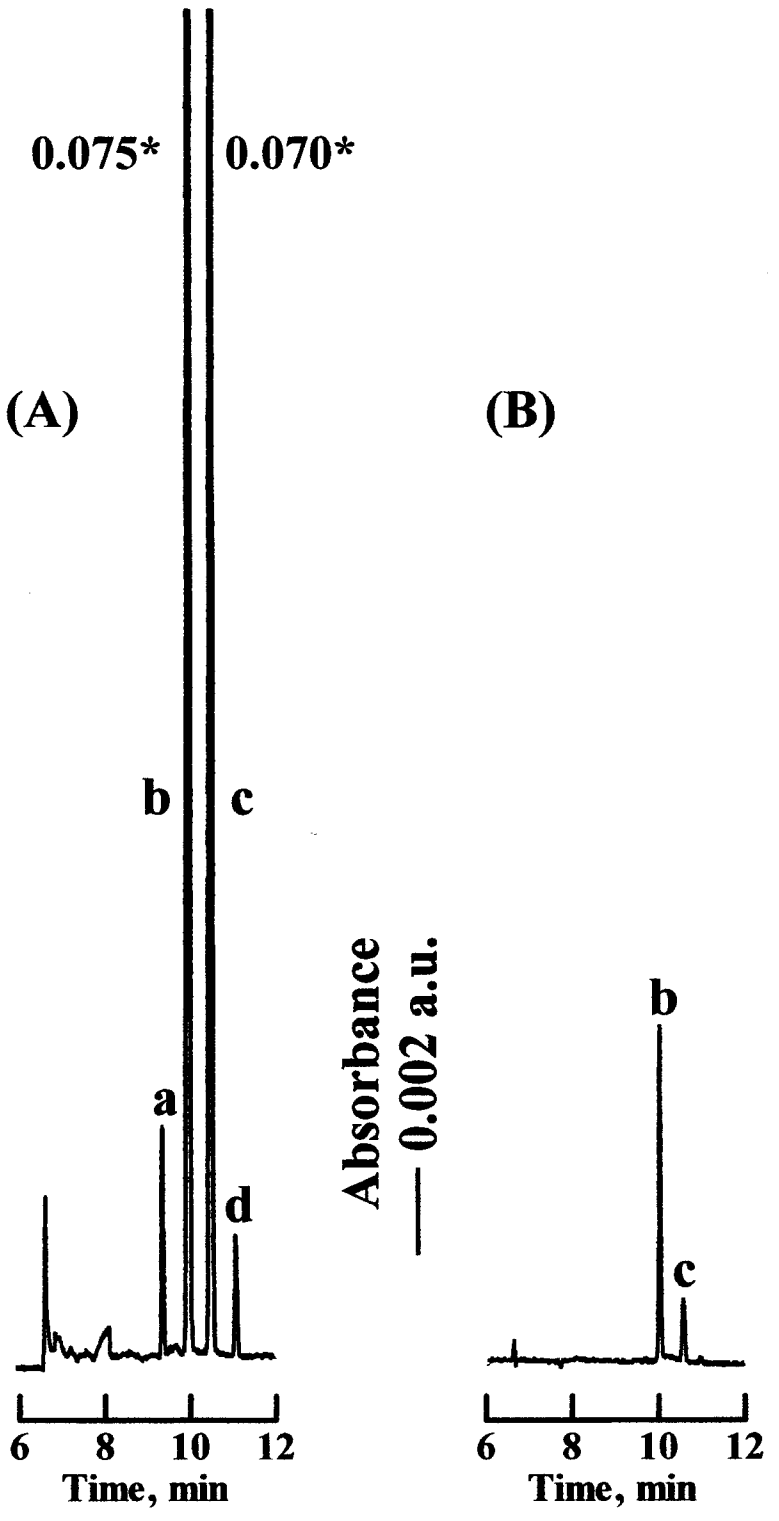

Figure 4. Effect of water plug for FASI on the peak height. (A) With water plug injected for 2 s. (B) Without water plug. Sample, 0.5 mg L^{-1} of each analyte in ACN. CZE conditions are as in Figure 1. Peak identification: a, phenol; b, PTPB; c, DPB; d, MPB.

However, the commercial triphenylborane is produced as pyridinyl complexes. Therefore, the second peak was assigned as PTPB instead of TPB. No peaks for MPB and phenol were observed in the case of the EKI (Figure 4(B)). A stronger electric field strength was necessary to introduce MPB and phenol into the capillary because the electrophoretic mobility for MPB and phenol in ACN are probably less than those for PTPB and DPB. The results show that the FASI performed on-column concentration for PTPB, DPB, MPB, and phenol.

3.5. Effect of electrode configurations

The effects of the vertical distance between the tip of electrode and the capillary end (D_{ec}) on the peak heights for the analytes were examined using optimum FASI conditions (water plug, 2 s; sample injection, 5 kV for 6 s), and the same samples as those described in the section "effect of water plug". The D_{ec} was set at 0.5 mm as a default D_{ec} or 8 mm (referred hereinafter as long D_{ec}). The electrode was moved upward to achieve the possible longest distance of 8 mm, at which the electrode remained situated in the 600 μL sample solution at a given vial volume 700 μL. The electrode tip was kept higher than the capillary end. Using a long D_{ec} (8 mm), the peak heights for PTPB and DPB were, respectively, 2.2 and 1.2 times higher than those obtained using the default D_{ec} (0.5 mm). The peak heights for MPB and phenol were, respectively, 0.41 and 0.40 times lower than those obtained using the default D_{ec}. Hirokawa *et al.* [37] determined atmospheric electrolytes using EKS-CZE with a default D_{ec} (1.1 mm) and a long D_{ec} (19.5 mm). The LODs obtained using the long D_{ec} were improved *ca.* five times in comparison with those by the default D_{ec}. In their procedure for anions, the pH of the BGE was 6.1 and the EOF

was suppressed using hydroxypropyl cellulose. During sample introduction, less analyte was moved back to the sample vial. In contrast, in our procedure, more analyte was moved back to the sample vial because of a strong EOF. This tendency for MPB and phenol was probably stronger than that for PTPB and DPB. A significant improvement was not obtained using the long D_{ec}. Therefore, the default D_{ec} was used further as the electrode configuration.

3.6. Calibration graphs

The Calibration graphs for PTPB, DPB, MPB, and phenol were linear using both the peak area and the peak height as the analytical response. Regression equations relating the height response (y) to the concentration for PTPB, DPB, MPB, and phenol (x, 0 – 300 μg L^{-1}) are shown in Table 1, which also presents the RSDs and LODs for the four analytes using the proposed FASI-CZE method. The RSDs of the peak area for PTPB, DPB, MPB, and phenol were obtained as 6.2 – 14%, for peak heights of 5.9 – 10%, and for migration times of 0.49 – 0.62%. The LODs obtained using the FASI-CZE were similar to those obtained using the HSIM-CZE [34]; the LODs of PTPB and DPB were *ca.* 30 times lower than those for the vacuum injection procedure, but the LODs of MPB and phenol were similar to those for the vacuum injection procedure [33]. The LOD for PTPB obtained using our method (0.85 μg L^{-1}) was superior to the LOD in the HPLC method by Oda *et al.* (810 μg L^{-1}) [28] and the LOD in the HPLC-MS method by Hanada *et al.* (12 μg L^{-1}) [29] although inferior to the LOD in the LC/MS/MS method by Tanaka *et al.* (68 pg L^{-1}) [40]. However, the LODs for MPB and phenol were 30 – 50 times higher than those for PTPB and DPB. Great room for improvement exists for the LODs for the

former analytes.

3.7. Applications

The proposed procedure was applied to the determination of PTPB, DPB, MPB, and phenol in the paint-waste samples obtained from shipyards. Figure 5 displays electropherograms of the analytes extracted from the paint wastes. Phenol, PTPB, and MPB were detected in waste I (Figure 5(I)), phenol and DPB were detected in waste II (Figure 5(II)), and all analytes were detected in waste III (Figure 5(III)) with the baseline separation. The electropherograms obtained for waste I, waste II, and waste III added with the standard of analytes are also shown (Figures 5(IA), (IIA), and (IIIA)). Table 2 presents analytical results for the analytes listed above in the samples using the standard addition method and the working curves. The former results agreed with the latter results. As a preliminary experiment, when a different paint-waste sample was analyzed using CZE with vacuum injection and HPLC [31], the concentration of PTPB (3.8 $\mu g\ g^{-1}$) found using the former agreed with that using the latter.

Table 1 Precision, LODs, and regression equations of PTPB, DPB, MPB, and phenol

Analyte	RSD (%[a])			LOD ($\mu g\ L^{-1}$, $S/N = 3$)		Regression equation (r, correlation coefficient)	Standard deviation	
	Area	Height	Time	FASI	HSIM[33]	Area (upper) and height (lower)	Slope	Intercept
PTPB	6.2	5.9	0.62	0.85	0.88	$y=9.72\times10^{5}x - 4.69\times10^{2}$ (r=0.9968)	4.91×10^{4}	3.60×10^{2}
						$y=2.79\times10^{5}x - 2.01\times10^{1}$ (r=0.9978)	1.74×10^{4}	1.61
DPB	14	10	0.56	0.88	1.0	$y=4.05\times10^{5}x+5.14\times10^{2}$ (r=0.9926)	2.08×10^{4}	1.92×10^{2}
						$y=2.28\times10^{5}x+7.82\times10^{1}$ (r=0.9927)	1.27×10^{4}	10.7
MPB	8.4	7.5	0.50	44	21	$y=1.46\times10^{4}x+1.03\times10^{2}$ (r=0.9983)	1.97×10^{2}	32.2
						$y=4.76\times10^{3}x - 4.88\times10^{1}$ (r=0.9745)	3.24×10^{2}	7.13
Phenol	9.6	6.8	0.49	28	23	$y=2.12\times10^{4}x - 1.02\times10^{2}$ (r=0.9967)	6.43×10^{2}	30.5
						$y=7.74\times10^{3}x - 9.83\times10^{1}$ (r=0.9970)	1.41×10^{2}	5.18

a. Sample: 0.030 mg L^{-1} of PTPB and DPB; 0.30 mg L^{-1} of MPB and phenol in ACN; n = 4. CZE conditions as in Fig. 4A.

b. In the regression equation, the x value is the concentration of analytes (0 – 0.030 mg L^{-1} of PTPB and DPB; 0 – 0.30 mg L^{-1} of MPB and phenol) and the y value is the peak area or height.

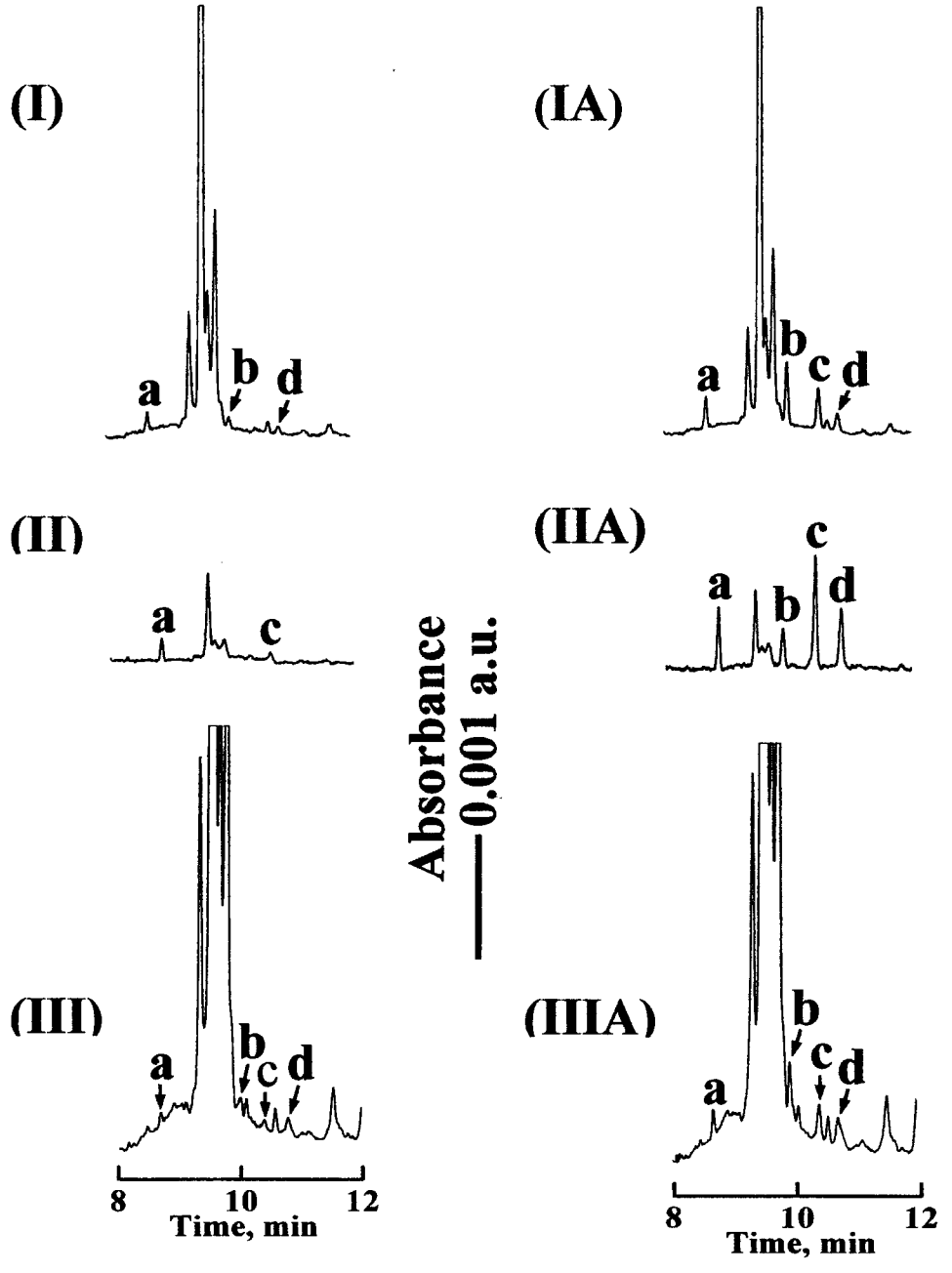

Figure 5. Electropherograms of paint-waste samples. (I) waste I, (IA) waste I added with 5 μg L^{-1} PTPB, DPB, 50 μg L^{-1} MPB, and phenol; (II) waste II, (IIA) waste II added with 10 μg L^{-1} PTPB, DPB, 100 μg L^{-1} MPB, and phenol; (III) waste III, (IIIA) waste III added with 5 μg L^{-1} PTPB, DPB, 50 μg L^{-1} MPB, and phenol. Peak identification: a, phenol; b, PTPB; c, DPB; d, MPB. CZE conditions are as presented Fig. 4(A).

Table 2 Analytical results for PTPB, DPB, MPB, and phenol in paint-waste samples obtained from shipyards[a]

Sample	Concentration ($\mu g\ g^{-1}$) ± standard deviation (n=3)							
	PTPB		DPB		MPB		Phenol	
	SA[b]	WC[c]	SA	WC	SA	WC	SA	WC
Waste I	0.076±0.010	0.048±0.002	ND[d]	ND	1.7±0.2	2.3±0.2	2.8±0.2	3.6±0.1
Waste II	ND	ND	0.015±0.001	0.021±0.001	ND	ND	1.2±0.1	1.6±0.02
Waste III	0.53±0.10	0.41±0.04	0.36±0.02	0.48±0.01	22±2	26±1	13±2	9.3±0.2

a. CZE conditions are as in Figure 4(A).

b. Concentrations were calculated using the peak height and standard addition (SA) procedure.

c. Concentrations were calculated using the peak height and the working curves (WC).

d. Not detected.

4. Conclusions

The CZE-FASI method was developed for the simultaneous determination of PTPB, DPB, MPB, and phenol. Under the optimized conditions, the peak heights for PTPB and DPB using the FASI were, respectively, 16 and 58 times higher than those obtained using the EKI (5 kV for 6 s). No peaks for MPB and phenol were observed in the case of the EKI. The LODs (at a *S/N* of 3) for PTPB, DPB, MPB, and phenol were, respectively, 0.85, 0.88, 44, and 28 μg L^{-1}. The RSDs (n = 4) for the analytes listed above were in the respective ranges of 6.2 – 14, 5.9 – 10, and 0.49 – 0.62% for the peak area, peak height, and migration time. The paint-waste samples were analyzed using FASI procedure, the concentrations of PTPB, DPB, MPB, and phenol in the paint-waste samples were 0.076 – 0.53, 0.015 – 0.36, 1.7 – 22, and 1.2 – 13 μg g^{-1}, respectively. This simple proposed method appears to be promising for the determination of PTPB and its degradation products in paint-waste samples. Further improvements of the LODs for MPB and phenol are expected to make the method more useful.

References

1. Xu, Z., Timerbaev, A. R., Hirokawa, T., *J. Chromatogr., A*, 2009, *1216*, 660-670.
2. Lee, I. S. L., Boyce, M. C., Breadmore, M. C., *Food Chem.* 2012, *133*, 205-211.
3. Kawai, T., Sueyoshi, K., Kitagawa, F., Otsuka, K., *Anal. Chem.* 2010, *82*, 6504-6511.
4. Kawai, T., Watanabe, M., Sueyoshi, K., Kitagawa, F., Otsuka, K. *J. Chromatogr. A*

2012, *1232*, 52-58.

5. Quirino, P., Haddad, P. R., *J. Sep. Sci.* 2011, *34*, 2872-2878.
6. Maijó, I., Borrull, F., Aguilar, C., Calull, M., *Chromatographia* 2011, *73*, 83-87.
7. Wang, C. C., Chen, C. C., Wang, S. J., Wu, S. M., *J. Chromatogr. A* 2011, *1218*, 6832-6837.
8. Jaafar, J., Irwan, Z., Ahamad, R., Terabe, S., Ikegami T., Tanaka, N., *J. Sep. Sci.* 2007, *30*, 391-398.
9. Kazarian, A. A., Hilder, E. F., Breadmore, M. C., *J. Sep. Sci.* 2011, *34*, 2800-2821.
10. Chien, R. L., Burgi, D. S., *J. Chromatogr.* 1991, *559*, 141-152.
11. Hu, X., Cui, S., Liu, J. Q., *Chromatographia* 2010, *72*, 993-997.
12. Hai, X., Nauwelaers, T., Busson, R., Adams, E., Hoogmartens, J., Schepdael, A. V., *Electrophoresis* 2010, *31*, 3352-3361.
13. Xu, L., Basheer, C., Lee, H. K., *J. Chromatogr. A* 2010, *1217*, 6036-6043.
14. Claude, B., Nehmé, R., Morin, P., *Anal. Chim. Acta* 2011, *699*, 242-248.
15. Liao, H. W., Lin, S. W., Wu, U. I., Kuo, C. H., *J. Chromatogr. A* 2012, *1226*, 48-54.
16. Hou, X., Deng, D., Wu, X., Lv, Y., Zhang, J., *J. Chromatogr. A* 2010, *1217*, 5622-5627.
17. Yu, L. S., Xu, X. Q., Huang, L., Lin, J. M., Chen, G. N., *Electrophoresis* 2009, *30*, 661-667.
18. Breadmore, M. C., *J. Chromatogr. A* 2010, *1217*, 3900-3906.
19. Quirino, J. P., *J. Sep. Sci.* 2011, *34*, 1020-1026.
20. Quirino, J. P., Breadmore, M. C., *J. Sep. Sci.* 2012, *35*, 60-65.
21. Dawod, M., Chung, D. S., *J. Sep. Sci.* 2011, *34*, 2790-2799.

22. Xu, Z., Kawahito, K., Ye, X., Timerbaev, A. R., Hirokawa, T., *Electrophoresis* 2011, *32*, 1195-1200.

23. Xu, Z., Nakamura, K., Timerbaev, A. R., Hirokawa, T., *Anal. Chem.* 2011, *83*, 398-401.

24. Dawod, M., Breadmore, M. C., Guijt, R. M., Haddad, P. R., *J. Chromatogr. A* 2009, *1216*, 3380-3386.

25. Zhang, H., Gavina, J., Feng, Y. L., *J. Chromatogr. A* 2011, *1218*, 3095-3104.

26. Meighan, M. M., Dawod, M., Guijt, R. M., Hayes, M. A., Breadmore, M. C., *J. Chromatogr. A* 2011, *1218*, 6750-6755.

27. Oukacine, F., Quirino, J. P., Garrelly, L., Romestand, B., Zou, T., Cottet, H., *Anal. Chem.*, 2011, *83*, 4949-4954.

28. Quirino, J. P., Aranas, A. T., *Anal. Chim. Acta*, 2012, *733*, 84-89.

29. Zhou, X., Okamura, H., Nagata, S., *Chemosphere* 2007, *67*, 1904-1910.

30. Oda, T., Sugawara, M., Nishino, S., *Annual Report of the Sapporo City Institute of Public Health*, 1998, 82-87.

31. Hanada, Y., Tanizaki, T., Koga, M., Shiraishi, H., Soma, M., *Anal. Sci.* 2002, *18*, 445-448.

32. Takahashi, K., Yoshikawa, E., Akiyama, M., Kitaori, K., Masuoka, S., *J. Jpn. Soc. Colour Mater.* 2005, *78*, 50-57.

33. Hsu, C. L. W., White, T. L., *J. Chromatogr. A* 1998, *828*, 461-467.

34. Fukushi, K., Yakushiji, Y., Okamura, H., Hashimoto, Y., Saito, K., *J. Chromatogr. A* 2010, *1217*, 2187-2190.

35. Kaewchuay, N., Yakushiji, Y., Fukushi, K., Saito, K., Hirokawa, T., *Electrophoresis* 2011, *32*, 1486-1491.

36. de Boer, T., Ensing, K., *J. Chromatogr. A* 1997, *788*, 212-217.

37. Hirokawa, T., Koshimidzu, K., Xu, Z., *Electrophoresis* 2008, *29*, 3786-3793.

38. Xu, Z., Koshimidzu, E., Hirokawa, T., *Electrophoresis* 2009, *30*, 3534-3539.

39. Cognetti, G., Maltagliati, F., *Mar. Pollut. Bull.* 2012, *64*, 175-176.

40. Supelco Solid Phase Extraction Products, Compilation prepared by Supelco Analytical, SIGMA-ALDRICH, http://www.supelco.com.tw/C-2%20%20150-163%20.New.pdf.

41. Tanaka, H., Hano, T., Kono, K., Inoue, T., *in Proceedings of the 21st Annual Symposium of Japan Society for Environmental Chemistry, Matsuyama*, 2012, 438.

Chapter 2

A Novel Hybrid Mode of Sample Injection to Enhance CZE Sensitivity for Simultaneous Determination of Pyridine-Triphenylborane Anti-Fouling Agent and Its Degradation Products

1. Introduction

CE is now a mature technique for separation-based analysis that implies several advantages, such as high separation efficiency, minimum requirements for sample and reagents, and (much) more rapid analysis, over other separation techniques [1]. A UV-vis absorbance detector is generally used in CE. However, the concentration sensitivity CE-UV is fairly poor because a small inner diameter of the capillary limits the optical path length for detection. Samples are conventionally injected into the capillary using hydrodynamic injection (HDI), *e.g.* under action of vacuum or pressure or electrokinetic injection (EKI). In addition to the conventional modes, different types of sample injection procedures have been proposed, including in-line sample concentration techniques, to enhance the CE sensitivity: large volume sample stacking [2-5], field-amplified sample injection (FASI) [6-16], ITP stacking [17, 18], ACN-mediated stacking [19-22], electrokinetic supercharging [23-28], *etc.* These procedures were shown to be effective but some of them were somewhat complicated in design and implementation.

As mentioned above, both the HDI and EKI are the most popular injection mode in CE and have different features [29]. A sample volume injected into the capillary can be

easily estimated for the HDI mode. In addition, any analytes including neutral, positive, and negative ones in spite of their actual mobilities can be introduced without changing the sample composition. However, with HDI severe zone broadening may occur due to a laminar flow generated during the injection [6]. On the other hand, in the EKI mode, it is more difficult to estimate the sample amount injected, because the actual amount is dependent on analyte mobilities and transport number of the analytes. In some analytical situation, this feature could be advantageous because analytes will be injected and then determined selectively. Importantly, the concentration stack is rather generated than the zone broadening when using EKI. However, its reproducibility is generally worse than that of HDI for the reasons discussed in ref. [30]. To underscore, each sample injection mode has its advantages and disadvantages. Therefore, it appears that if the sample can be injected using both modes simultaneously, a combined injection mode could produce certain gains by taking advantages of individual injection modes, especially when the sample contains ions, which have higher and lower mobilities simultaneously as in the present case.

An anti-fouling agent is usually applied to ship hulls to prevent worsening of fuel consumption rates resulting from the buildup of marine organisms, such as barnacles and bivalves, which with time become attached to the surfaces of ship hulls. One anti-fouling agent, pyridine-triphenylborane (PTPB), is frequently used in some Asian countries because of its proven effectiveness [31]. In order to elucidate its degradation products and their toxicities to marine organisms, it is important to develop an analytical method for these compounds. We have previously developed a CZE method with direct UV detection for the simultaneous determination of PTPB and its degradation products such as diphenylborinic acid (DPB), phenylboronic acid (MPB), and phenol [32]. Additional

improvement of the LODs is desirable for making the quantification of lower concentrations of these compounds feasible and thus the method more useful. In the present study, we proposed a novel hybrid sample injection mode (HSIM) which was the combination of vacuum injection and EKI to improve sensitivity. In this way, samples were introduced into the capillary using both vacuum and EKI simultaneously, with a short water plug injected into the capillary prior to sample introduction. Using a sample mixture containing PTPB, DPB, MPB, and phenol in ACN, injection conditions (time of water plug injection, time, voltage of sample introduction *etc.*) were examined and optimized. The performance of the proposed HSIM was compared with the conventional sample injection modes. Tůma *et al.* mentioned that the sample could be electrokinetically and hydrodynamically injected into the capillary if the split-flow injector was used with the capillary inlet oriented against the BGE flow [33]. However, this geometric arrangement was not tested further. To the best of our knowledge, the present study might be the first attempt to use different injection modes simultaneously as a simple procedure to enhance the CZE sensitivity.

2. Experiments

2.1. Apparatus

The CE apparatus used throughout this study was equipped with a UV-vis absorbance detector (270A-HT; Perkin-Elmer, Foster City, CA, USA). Usually, in this apparatus samples can be introduced into the capillary either electrokinetically or by applying vacuum. However, it was also possible to introduce samples using both vacuum injection and EKI simultaneously. The rise time for the detector was set at 0.5 s. A

polyimide-coated fused-silica capillary column was used (75 μm i.d. × 375 μm o.d.; GL Sciences, Tokyo, Japan). The total length of the column was 72 cm; its effective length was 50 cm. The peak area, peak height, and migration time were measured using a Chromato-Integrator (D-2500; Hitachi, Tokyo, Japan). The pH measurements were carried out using a pH meter (F-22; Horiba, Kyoto, Japan).

2.2. Reagents

All reagents were of analytical-reagent grade and used as received. Pyridine-triphenylborane, diphenylborinic acid, and phenylboronic acid were obtained from Hokko Chemical (Tokyo, Japan). Phenol was the product of Nacalai Tesque (Kyoto, Japan). The individual stock solutions (1000 mg/L) of PTPB, DPB, MPB, and phenol were prepared in ACN purchased from Nacalai Tesque. To keep the stability of stock solutions for a longer time, 1% (v/v) pyridine (Nacalai Tesque) was added and the solutions were then covered with an aluminum foil and kept at 4°C to prevent their degradation. Standard solutions used for the examination of analytical conditions and building-up the calibration graphs were prepared by serial dilutions of stock solutions with ACN. The pH of the BGE (a 20 mM solution of sodium tetraborate) was adjusted pH 9.8 using 1 M NaOH (Nacalai Tesque). The BGE was filtered through a 0.45 μm membrane filter (Advantec Toyo Kaisha, Tokyo, Japan) before use. Distilled, deionized water, obtained from an automatic still (WG220; Yamato Kagaku, Tokyo, Japan) and a Simpli Lab-UV high-purity water apparatus (Nihon Millipore, Tokyo, Japan) was used throughout.

2.3. CZE Procedure

New capillaries were pretreated by flushing with 1 M NaOH for 40 min and then with water for 10 min. Before the first analysis of each day, the capillary was washed with water for 5 min, 1 M NaOH for 5 min, and water for 10 min. The detection wavelength was set at 200 nm. The capillary was thermostated at 30°C. The following optimum analytical conditions were established. Between runs, the capillary was flushed with 0.1 M NaOH for 3 min, and then filled with the BGE for 3 min. After that, water was injected by applying vacuum (16.9 kPa) for 1 s (corresponding to 21 nL) and the sample solution was injected into the capillary using both vacuum and voltage (4 kV for 4 s, at a negative polarity at the capillary inlet end) simultaneously. A positive voltage of 15 kV was applied for separation. Each step was run automatically. After each analysis, 700 μL of the sample was newly filled in the sample vial. Calibration graphs were prepared using synthetic standards.

Electrophoretic mobilities were calculated as follows [34]:

$$\mu_{ep} = \mu_a - \mu_{eof} \quad (1)$$

$$\mu_a = lL / t_a V \quad (2)$$

$$\mu_{eof} = lL / t_{eof} V \quad (3)$$

where μ_{ep} is electrophoretic mobility of an analyte, μ_a apparent mobility, μ_{eof} is the EOF mobility, l is effective length of the capillary, L total length of the capillary, t_a the migration time of the analyte, V the applied voltage, and t_{eof} the migration time of EOF marker. The first peak in electropherograms that corresponds to acetonitrile or pyridine

was used as the EOF marker to calculate the EOF mobility.

3. Results and discussion

3.1. Sample injection mode

Schematics of sample injection modes generally used in CE is illustrated in Figure 1. Any analytes including neutral, positive, and negative ones regardless of their actual mobilities can be introduced using HDI (Figure 1A). On the other hand, either positive or negative analytes can only be injected using EKI (Figure 1B) if the EOF is negligible or suppressed. In order to improve the sensitivity and reproducibility of EKI, a short water plug is injected into the capillary prior to sample introduction (FASI, Figure 1C). Analytes are then stacked around the interface between BGE and the water plug. We proposed here a new sample introduction procedure, HSIM, which was the combined sample introduction mode of HDI and EKI. Using HSIM (Figure 1D), any analytes can be introduced similarly to HDI, but increased amounts of charged analytes (either cations or anions) are injected compared to those using single HDI. Furthermore, a part of charged analytes may be stacked at the beginning of HSIM because of high electric field. The analytes in the present study were anions, which moved to the detector end because of higher EOF after the sample was introduced using HSIM, as shown in Figure 1E.

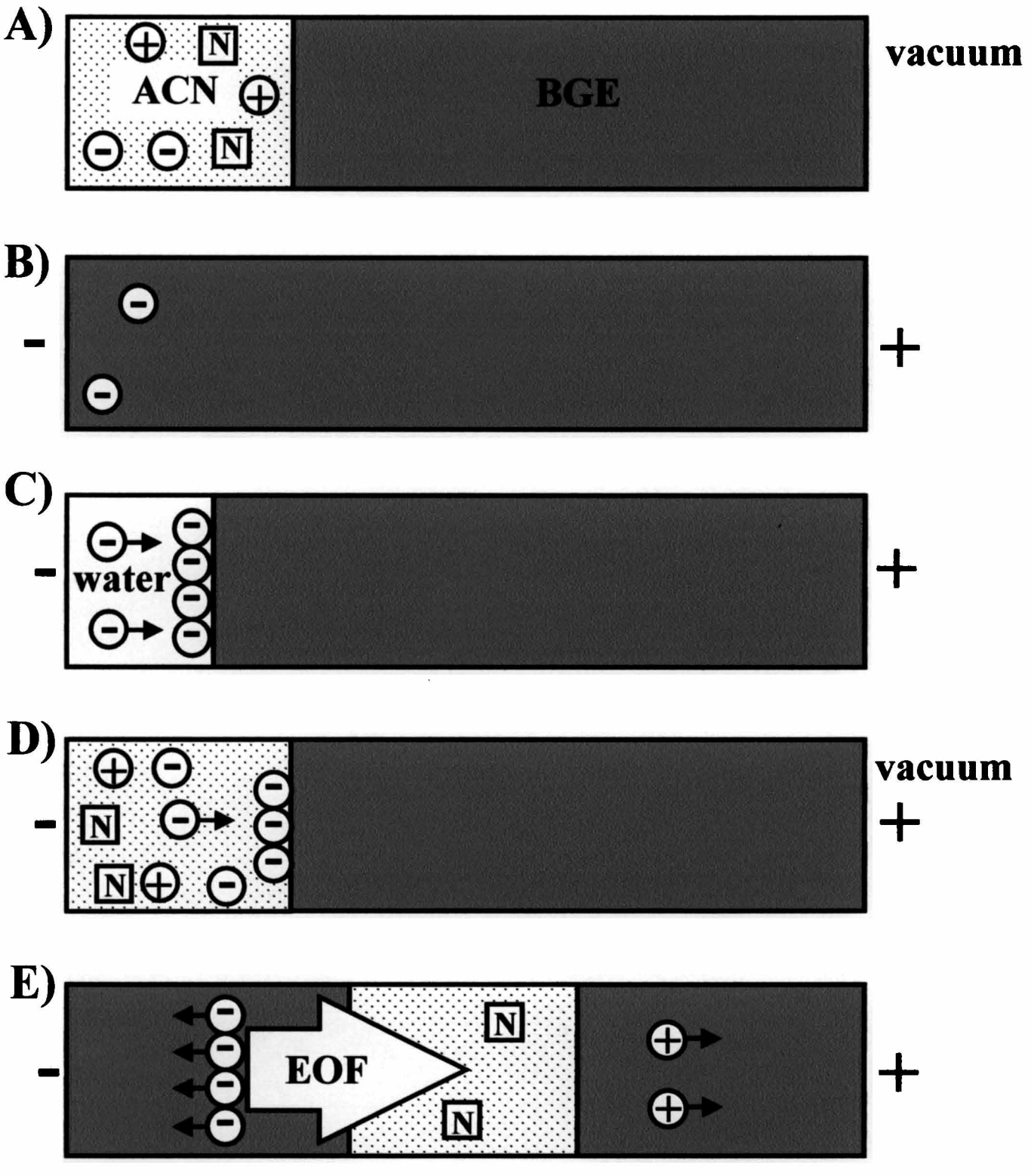

Figure 1. Schematics of sample injection modes. (A) HDI (vacuum), (B) EKI, (C) FASI, (D) HSIM, (E) migration of analytes for HSIM. ACN, sample solvent; +, cation; -, anion; N, neutral species.

3.2. Sensitivity enhancement potential of HSIM

To verify the sensitivity enhancement potential of HSIM regarding PTPB, DPB, MPB, and phenol, the following experiments were carried out. A mixture of 0.4 mg/L PTPB, DPB, MPB, and phenol were analyzed using three modes of injection and the results are compared in Figure 2. Peak heights for PTPB, DPB, MPB, and phenol notably increased using HSIM with an enhancement factor of 12, 12, 1.5, and 1.3, respectively, compared to vacuum injection (cf. Figures 2(C) and 2(A)). The sample was also injected using EKI immediately after vacuum injection (Figure 2(B)) and peak heights using HSIM increased by a factor of 5.2, 3.3, 2.2, and 1.2, respectively, were observed in comparison with the results obtained by the successive injection. It was presumed that a sufficient amount of analytes could not move across the boundary between essentially nonaqueous sample zone and aqueous BGE zone because of the lack of current in the case of successive injection. When the sample was injected using only EKI, no peaks were observed. In general, it is difficult to introduce extremely low-mobility ions and neutral species into the capillary using the EKI mode without applying a correct polarity voltage to generate EOF. However, both higher and lower-mobility ions and neutral species can be simultaneously injected using HSIM. It was deemed that HSIM would be a promising sample injection mode for samples, which contain both ionic and nonionic substances. Therefore, the following experiments were performed in order to establish optimum HSIM conditions.

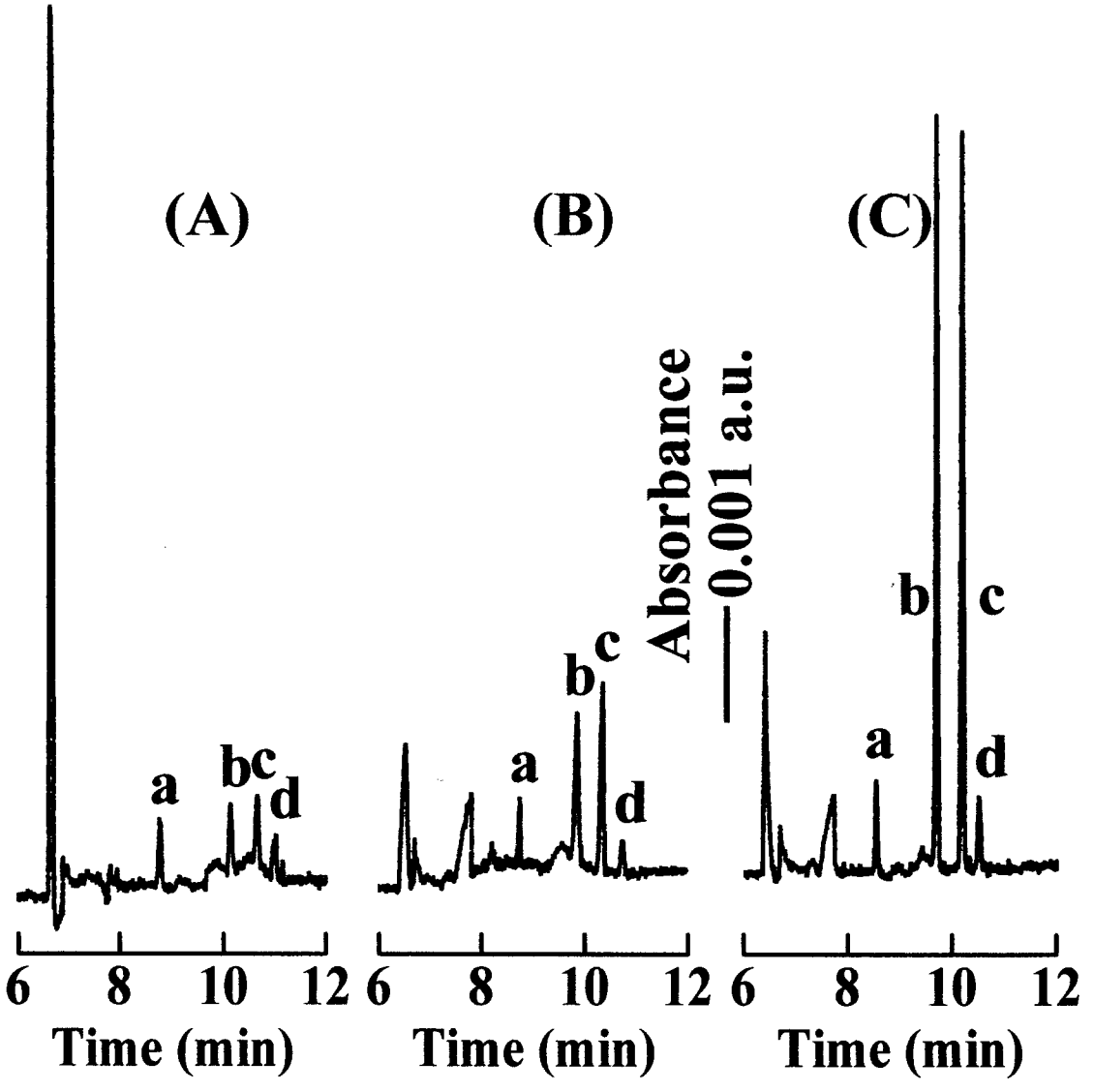

Figure 2. Electropherograms of a standard solution of phenol, PTPB, DPB, and MPB obtained with different injection modes. (A) Vacuum injection for 1 s (21 nL); (B) vacuum injection for 1 s and then electrokinetic injection at 1 kV for 1 s; (C) HSIM at 1 kV for 1 s. CZE conditions: capillary, 50/72 cm × 75 μm i.d.; BGE, 20 mM sodium tetraborate adjusted to pH 9.8 with 1 M NaOH; voltage, 15 kV; wavelength for detection, 200 nm. Sample, 0.4 mg L^{-1} of each analyte in ACN. Peak identification: a, phenol; b, PTPB; c, DPB; d, MPB.

3.3. Effect of water plug

It was reported that the sensitivity and reproducibility could be improved by injecting a water plug into the capillary prior to EKI (*i.e.* using FASI) [22]. Therefore, the injection time for the water plug was varied between 0 and 2 s using HSIM. As can be seen from Figure 3, the peak height for PTPB decreased with increasing injection time. Also, the highest peak was obtained for DPB when the injection time was 1 s, whereas for phenol the peak height increased with the injection time up to 0.5 s, leveled off around 0.5–1.5 s, and then decreased. The peak height for MPB was almost constant up to 1.5 s and then decreased. When the injection time was 1 s, the RSDs of peak heights for PTPB, DPB, MPB, and phenol were in the range from 3.7 to 9.2%. The RSDs for 1-s injections were almost the same as those for 1.5 s (2.9–8.3 s), smaller than those for 0.5 s (6.2–37%), 2 s (5.1–10%), and without the water plug (3.4–22%). Therefore, optimum injection time of the water plug adopted in the subsequent experiments was 1 s.

3.4. Effect of sample-injection time

The sample injection time was varied between 1 and 5 s using HSIM. The peak height for PTPB increased with the injection time up to 2 s, almost leveled off when going to 4 s, and then declined. The peak height for DPB was almost constant with the injection time up to 5 s. The peak height for MPB increased with the injection time up to 3 s and almost leveled off. The peak height for phenol increased up to an injection time of 5 s. The baseline separation was not observed for PTPB and DPB at 5 s. On the other hand, the RSDs of peak height for all analytes at the sample injection time in the range of 1–4 s

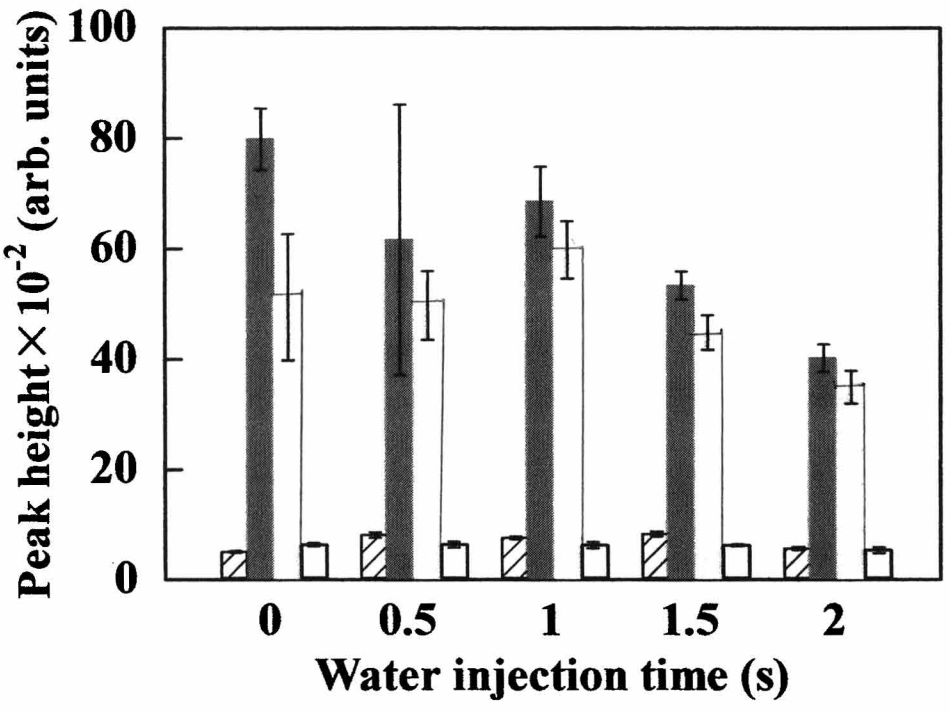

Figure 3. Effect of injection time of water plug on the peak height. Each bar corresponds to phenol, PTPB, DPB, and MPB, respectively, from left to right. Sample, 0.4 mg L^{-1} of each analyte in ACN. Injection: HSIM at 1 kV for 1 s. Other conditions as in Figure 2.

were 7.1–13, 5.2–12, 5.6–14, and 1.6–9.3%, respectively. Therefore, 4 s was chosen as the optimum sample injection time.

3.5. Effect of sample-injection voltage

The injection voltage was varied between 1 and 5 kV using HSIM with the sample injection time for 4 s. The results are illustrated in Figure 4. The peak height for PTPB, DPB, and MPB increased with increasing the injection voltage up to 4 kV and then decreased. The peak height for phenol was almost constant up to 4 kV and then decreased. The RSDs of peak height for the sample injection voltage ranged from 1 to 4 kV were 1.6–9.3, 2.2–11, 1.8–13, and 2.9–9.5%, respectively. Therefore, 4 kV was further used as the optimum injection voltage. Peak heights for PTPB, DPB, MPB, and phenol using HSIM at 4 kV for 4 s (Figure 5B) were 30, 22, 1.8, and 1.0 times higher, respectively, when compared to the results obtained with only vacuum injection for 4 s (Figure 5(A)). The peak heights of MPB and phenol obtained using HSIM were much lower than that of PTPB or DPB. In order to elucidate the reasons, the electrophoretic mobilities of PTPB, DPB, MPB, and phenol in the BGE (pH 9.8) were calculated using the procedure described in Section 2.2.3. The results were 15.8×10^{-5}, 17.3×10^{-5}, 18.3×10^{-5}, and 12.4×10^{-5} $cm^2V^{-1}s^{-1}$, respectively; the EOF was 52.2×10^{-5} $cm^2V^{-1}s^{-1}$. There was not much difference among these electrophoretic mobilities. The electrophoretic mobilities of MPB and phenol in the sample solution prepared using ACN are probably lower than those in the aqueous BGE (pH 9.8). In addition, molar absorptivities for PTPB, DPB, MPB, and phenol were estimated as 2.3×10^5, 9.2×10^4, 5.2×10^4, and 6.5×10^4 $lmol^{-1}cm^{-1}$, respectively (for example, concentration of PTPB was 1.56×10^{-6} M, absorbance

2.64×10^{-3}, optical path length 7.5×10^{-3} cm, giving a molar absorptivity of 2.3×10^{5}). The molar absorptivities for MPB, phenol, and DPB were 77, 72, and 60% lower than that for PTPB, respectively. The differences were another reason for the lower peak heights for MPB and phenol.

Charge states for the four analytes of interest were presumed as follows. As mentioned in our previous paper [32], MPB changed to an anion type under a basic condition because of the coordination of the hydroxide ion to the boron. It can be presumed that the charge state for MPB is −1 in the BGE (pH 9.8) because of its pK_a value (8.8) [35, 36]. The chemical form of PTPB in water was supposed to be mainly triphenylborate after liberating pyridine. Probably, the coordination of the hydroxide ion could be happened in the cases of PTPB and DPB, similarly to MPB. It can be also presumed that the charge state for DPB is −1 in due account of its pK_a value (6.2) [36, 37]. The charge state for PTPB seems to be similar to other analytes although the pK_a of PTPB is unknown. On the other hand, the charge state for phenol could be −1 because of its p*K*a value (10) [38].

3.6. Calibration graphs

Calibration graphs for PTPB, DPB, MPB, and phenol were linear using both the peak area and peak height as analytical response. Regression equations relating the area or height response (y) to concentration for PTPB, DPB, MPB, and phenol (x, 0–0.1 mg L^{-1}) are accommodated in Table 3.1. Table 3.1 presents also the RSDs, LODs, and regression equation for the four analytes using the proposed HSIM-CZE method. The RSDs (intra-day) of peak area for PTPB, DPB, MPB, and phenol were obtained as

Table 1 Precision, LODs, and regression equation of PTPB, DPB, MPB, and phenol using HSIM

Analyte	RSD (intraday, %)[a]			LOD ($\mu g\ L^{-1}$, $S/N = 3$)		Regression equation[c] (correlation coefficient)	
	Area	Height	Time	HSIM	Vacuum[b]	Area	Height
PTPB	7.1	5.7	0.49	0.88	25	$y = 1.59\times10^{3}x$-6.43 (0.9967)	$y = 3.62\times10^{2}x$ -0.995 (0.9965)
DPB	1.9	4.3	0.43	1.0	30	$y = 7.65\times10^{2}x$+0.419 (0.9799)	$y = 1.68\times10^{2}x$+0.208 (0.9872)
MPB	7.8	6.8	0.34	21	50	$y = 62.2x$-0.246 (0.9855)	$y = 14.3x$-0.0421 (0.9925)
Phenol	11	9.2	0.66	23	29	$y = 26.2x$+0.305 (0.9719)	$y = 7.63x$+0.0590 (0.9889)

a) Sample: 0.04 mg L^{-1} of PTPB, DPB, MPB, and phenol in ACN; $n = 4$. CZE conditions as in Fig. 5B.

b) At 4 s.

c) In the regression equation, the x value is the concentration of analytes (0–0.1 mg L^{-1}), the y value is the peak area / peak height.

1.9–11%, for peak heights 4.3–9.2%, and for migration times 0.34–0.66%. The LODs were improved 35, 30, 2.4, and 1.2 times for PTPB, DPB, MPB, and phenol compared to the LODs obtained using vacuum injection.

4. Conclusions

A novel method HSIM that presents the combination of electrokinetic injection (EKI) and vacuum injection was developed to enhance detection sensitivity in CZE. Samples were introduced using both vacuum and electrokinetic injections simultaneously, with a water plug injected into the capillary prior to sample introduction (i.e., similarly to field amplified sample injection, FASI). The signal intensity (peak height) was found to be up to a 30-fold increased using HSIM by applying 4 kV for 4 s at the inlet end of the capillary as the cathode with supplementary vacuum in comparison with only vacuum injection for 4 s. The RSDs (n = *4*, intra-day) for the above analytes were in the ranges of 1.9–11%, 4.3–9.2%, and 0.34–0.66% for peak area, peak height, and migration time, respectively. The LODs (at a *S/N* of 3) for PTPB, DPB, MPB, and phenol were, 0.88, 1.0, 21, and 23 μg L^{-1}, respectively. The HSIM is a simple and a promising procedure to be useful for enhancing the sensitivity for both low-and high-mobility ions in CZE.

References

1. Zheng, L., Zhang, L., Tong, P., Zheng, X., Chi, Y., Chen, G., *Talanta* 2010, *81*, 1288-1294.

2. Quirino, J. P., Terabe, S., *J. Chromatogr. A* 1999, *850,* 339-344.

3. Chun, M. S., Chung, D. S., *Anal. Chim. Acta* 2003, *491*, 173-179.

4. Quesada-Molina, C., García-Campaña, A. M., del Olmo-Iruela, L., del Olmo, M., *J. Chromatogr. A* 2007, *1164,* 320-328.

5. Honger, J., Šafra, J., Polášek, M., Pospíšilová, M., *Chromatographia* 2010, *72*, 885-891.

6. Chien, R. L., Burgi, D. S., *J. Chromatogr.* 1991, *559*, 141-152.

7. Li, K., Li, S. F. Y., *Analyst* 1995, *120*, 361-366.

8. Zhang, C. X., Thormann, W., *Anal. Chem.* 1996, *68*, 2523-2532.

9. Martínez, D., Borrull, F., Calull, M., *J. Chromatogr. A* 1997, *788*, 185-193.

10. Zhang, L. Y., Sun, M. X., *J. Chromatogr. A* 2005, *1100*, 230-235.

11. Hernández-Borges, J., Gracía-Montelongo, F. J., Cifuentes, A., Rodríguez-Delgado, M. Á., *J. Chromatogr. A* 2005, *1100*, 236-242.

12. Weng, Q., Xu, G., Yuan, K., Tang, P., *J. Chromatogr. B* 2006, *835*, 55-61.

13. Huhn, C., Pyell, U., *J. Chromatogr. A* 2010, *1217*, 4476-4486.

14. Xu, L., Basheer, C., Lee, H. K., *J. Chromatogr. A* 2010, *1217*, 6036-6043.

15. Breadmore, M. C., Quirino, J. P., *Anal. Chem.* 2008, *80*, 6373-6381.

16. Hu, X., Cui, S., Liu, J. Q., *Chromatographia* 2010, *72*, 993-997.

17. Breadmore, M. C., *Electrophoresis* 2008, *29*, 1082-1091.

18. Breadmore, M. C., *J. Chromatogr. A* 2010, *1217*, 3900-3906.

19. Shihabi, Z. K., *Electrophoresis* 1998, *19*, 3008-3011.

20. Shihabi, Z. K., *Electrophoresis* 2002, *23*, 1612-1617.

21. Kubalczyk, P., Bald, E., *Electrophoresis* 2008, *29*, 3636-3640.

22. Yu, L. S., Xu, X. Q., Huang, L., Lin, J. M., Chen, G. N., *Electrophoresis* 2009, *30*,

661-667.

23. Hirokawa, T., Okamoto, H. Gaš, B., *Electrophoresis* 2003, *24*, 498-504.

24. Xu, Z., Koshimidzu, E., Hirokawa, T., *Electrophoresis* 2009, *30*, 3534-3539.

25. Lu, Y., Breadmore, M. C., *J. Sep. Sci.* 2010, *33*, 2140-2144.

26. Botello, I., Borrull, F., Aguilar, C., Calull, M., *Electrophoresis* 2010, *31*, 2964-2973.

27. Lu, Y., Breadmore, M. C., *J. Chromatogr. A* 2010, *1217*, 7282-7287.

28. Xu, Z., Nakamura, K., Timerbaev, A. R., Hirokawa, T., *Anal. Chem.* 2011, *83*, 398-401.

29. Krivácsy, Z., Gelencsér, A., Hlavay, J., Kiss, G., Sárvári, Z., *J. Chromatogr. A* 1999, *834*, 21-44.

30. de Boer, T., Ensing, K, *J. Chromatogr. A* 1997, *788*, 212-217.

31. Zhou, X., Okamura, H., Nagata, S., *Chemosphere* 2007, *67*, 1904-1910.

32. Fukushi, K., Yakushiji, Y., Okamura, H., Hashimoto, Y., Saito, K., *J. Chromatogr. A* 2010, *1217*, 2187-2190.

33. Tůma, P., Opekar, F., Jelínek, I., *J. Chromatogr. A* 2000, *883*, 223-230.

34. Heiger, D. N., *Capillary Denki-Eido Nyumon*, Agilent Technologies, Tokyo 1994, pp. 18-19.

35. Yan, J., Springsteen, G., Deeter, S., Wang, B., *Tetrahedron* 2004, *60*, 11205-11209.

36. Morin, G. T., Hughes, M. P., Paugam, M. F., Smith, B. D., *J. Am. Chem. Soc.* 1994, *116*, 8895-8901.

37. Steiner, S. J., Bien, J. T., Smith, B. D., *Bioorg. Med. Chem. Lett.* 1994, *4*, 2417-2420.

38. Canals, I., Bosch, E., Rosés, M., *Anal. Chim. Acta* 2002, *458*, 355-366.

39. Hirokawa, T., Koshimidzu, E., Xu, Z., *Electrophoresis* 2008, *29*, 3786-3793.

Chapter 3

Simultaneous Determination of Pyridine-Triphenylborane Anti-Fouling Agent and Its Degradation Products in Artificial Seawater Using Capillary Zone Electrophoresis and Evaluation for Degradation of Pyridine-Triphenylborane

1. Introduction

Anti-fouling agents, which are harmful to non-target marine organisms, are usually applied to ship hulls and fishnets to prevent biofouling in seawater [1]. Such agents generally degrade to other compounds after dissolution into seawater. One anti-fouling agent, pyridine-triphenylborane (PTPB), is popularly used in some Asian countries including Japan because of its effectiveness [2]. Several reports have described the degradation process of PTPB, in addition to its degradation products and their toxicities to marine organisms [1–4]. Conventionally, analytical methods such as HPLC and HPLC-MS have been used for determination of PTPB and its degradation products diphenylborinic acid (DPB), phenylboronic acid (MPB), and phenol from acetonitrile (ACN) extracts from artificial seawater (ASW) and natural seawater [1–7]. When using such methods, PTPB and its degradation products can not be determined simultaneously. Extraction must be repeated. This important shortcoming is regarded as one reason why degradation products and their toxicities remain poorly understood. It is therefore worthwhile to develop a method involving no extraction procedure for simultaneous

determination of these compounds in seawater.

We previously developed a CZE with direct UV detection for the simultaneous determination of PTPB, DPB, and phenol prepared in acetonitrile (ACN) [8–10]. Simple degradation experiments using ACN solutions containing PTPB were also conducted to verify the usefulness of the proposed method [8]. In this study, we modified this method to determine PTPB, DPB, MPB, and phenol dissolved in artificial seawater (ASW) directly with no extraction procedure. In this case, it is necessary to prevent interference from high matrix components such as chloride in the ASW solutions. In the previous method, voltage was applied with the sample inlet side as the anode to migrate the analytes after samples were vacuum injected into the capillary. It was expected that high concentrations of chloride in the ASW samples could be moved back to the sample inlet side during migration because of its high electrophoretic mobility. Consequently, the interference can be reduced and the separation of the analytes can be expected to be consequently improved. Using the same procedures for the sample injection and voltage application, the following analytical conditions were examined: background electrolyte (BGE) concentration, ACN concentration in ASW sample solutions, and sample-injection time. In addition, degradation experiments using the ASW sample solutions containing PTPB were conducted similarly to the former experiments. This report is the first of an attempt to determine PTPB, DPB, MPB, and phenol in ASW with no sample extraction procedure.

2. Experiments

2.1. Apparatus

The CE apparatus used throughout this study was equipped with a UV–Vis absorbance detector (270A-HT; PerkinElmer Inc., Foster City, CA). The rise time for the detector was set at 0.5 s. A polyimide-coated fused-silica capillary was used (75 μm ID × 375 μm OD; GL Sciences Inc., Tokyo, Japan). The total capillary length was 72 cm; its effective length was 50 cm. The peak area, peak height, and migration time were measured using a Chromato-Integrator (D-2500; Hitachi Ltd., Tokyo, Japan). The pH measurements were conducted using a pH meter (F-22; Horiba Ltd., Kyoto, Japan).

2.2. Reagents

All reagents were of analytical-reagent grade and were used as received. PTPB, DPB, and MPB were obtained from Hokko Chemical Ind. Co. Ltd. (Tokyo, Japan). Phenol was the product of Nacalai Tesque Inc. (Kyoto, Japan). Individual stock solutions (1000 mg L^{-1}) of PTPB, DPB, MPB, and phenol were prepared in acetonitrile (ACN) purchased from Nacalai Tesque Inc. To maintain their stability, 1% (v/v) pyridine (Nacalai Tesque Inc.) was added to the stock solutions except for phenol. The solutions were then covered with aluminum foil and kept at 4°C to prevent their degradation. Standard solutions used for the examination of analytical conditions and building-up of calibration graphs were prepared by mixing diluted stock solutions with ACN and artificial seawater (ASW). The preparation of ASW was based on the Japanese Standard [11]. The pH of the BGE (a 60-mM solution of sodium tetraborate) was adjusted to 9.8 using 1 M NaOH (Nacalai Tesque Inc.). The ASW and the BGE were filtered through a 0.45-μm membrane filter (Advantec Toyo Kaisha Ltd., Tokyo, Japan) before use. Distilled, deionized water, obtained from an automatic still (WG220; Yamato Kagaku Co.

Ltd.) and a Simpli Lab-UV high-purity water apparatus (Merck Millipore, Tokyo, Japan) were used throughout.

2.3. CZE procedure

New capillaries were pretreated by flushing with 1 M NaOH for 40 min and then with water for 10 min. Before the first analysis of each day, the capillary was washed with water for 5 min, 1 M NaOH for 5 min, and water for 10 min. The capillary was thermostated at 30°C. The detection wavelength was set at 200 nm. It was then filled with the BGE (a 60-mM solution of sodium tetraborate adjusted to 9.8 using 1 M NaOH) for 3 min. The sample solution was injected by application of a vacuum (16.9 kPa) for 4 s (corresponding to 84 nL). A positive voltage of 15 kV was applied for separation. Between runs, the capillary was flushed with 0.1 M NaOH for 3 min. Each step was run automatically. The capillary was flushed with water for 5 min to fill the capillary with water at the end of the day. Calibration graphs were prepared using synthetic standards.

2.4. Degradation experiments

A 1000 mg L^{-1} PTPB in ACN solution without pyridine was prepared immediately before degradation experiments. Then 500 mL of ASW solution containing 1.0 mg L^{-1} PTPB was prepared using the solution above. Into each of 30 screw-top glass test tubes (10.8 mm ID × 10-mm-long), 7 mL of the solution was put. Then 10 test tubes each were put into three conditions: open air (started at the beginning of August on the rooftop with 34°C average temperature), a room with light (turning on ceiling fluorescent lamps for

only daytime, 25°C), and a room without light (in a plastic box with a lid, 25°C). Some test tubes were collected from the three conditions over time. Before ascertaining the concentrations of PTPB and its degradation products in the sample solutions using the proposed method, 20% (v/v) ACN and 0.003% pyridine were added to the solutions. The concentrations were calculated using calibration graphs of the peak area.

3. Results and discussion

3.1. Effect of the BGE concentration

A mixture of 1.0 mg L^{-1} PTPB, DPB, MPB, and phenol in ASW was analyzed to examine the effects of BGE concentration on the separation behavior. The BGE (sodium tetraborate) concentration was varied between 20 and 60 mM. The results are presented for comparison in Figure 1. When 20 mM BGE was used, the peaks of PTPB, DPB, and MPB could not be separated, although phenol was detected separately (Figure 1A). Separation for all analytes was improved with increasing concentration of BGE up to 60 mM. The analysis time was prolonged. This improvement can result from reduced EOF with increased buffer concentration [12]. In spite of the higher concentration of chloride in the sample solution, four analyte peaks were clearly observed (Figure 1D). Simulation results obtained using Simul 5 introduced by Gaš et al. [13] suggested that chlorides, which have higher effective mobility than the EOF mobility, were moved back to the sample inlet side during migration. However, the effective mobilities of the analytes were lower than the EOF mobility [9]. Therefore, the analytes were roughly separated without being severely affected by the chloride. In addition, the sharp phenol peak was observed because of the stacking effect caused by a pH junction [14]. When higher BGE

concentration (> 60 mM) was used, an unstable baseline with higher noise was observed (result not shown). Therefore, the optimum concentration of the BGE adopted in the subsequent experiments was 60 mM.

3.2. Effect of concentration of acetonitrile in sample solutions

Results show that when samples contain both chloride and ACN, sample stacking can result from transient "pseudo-isotachophoresis" (pseudo-ITP): chloride and ACN respectively act as leading and terminating ions [15]. Therefore, the amount of ACN in the ASW solution containing 1.0 mg L^{-1} PTPB, DPB, MPB, and phenol, was varied between 0 and 30% (v/v). As might be apparent from Figure. 2, the peaks for PTPB, DPB, and MPB sharpened with increasing amount of ACN up to 20% (v/v). When the amount of ACN was 30% (v/v) (Figure 2D), no marked improvement was observed, but the migration time increased. Furthermore, the addition of ACN into samples results in the dilution of the samples. The dilution of samples should be avoided for the determination of lower concentrations of analytes. Therefore, 20% (v/v) was chosen as the optimum ACN concentration in ASW samples.

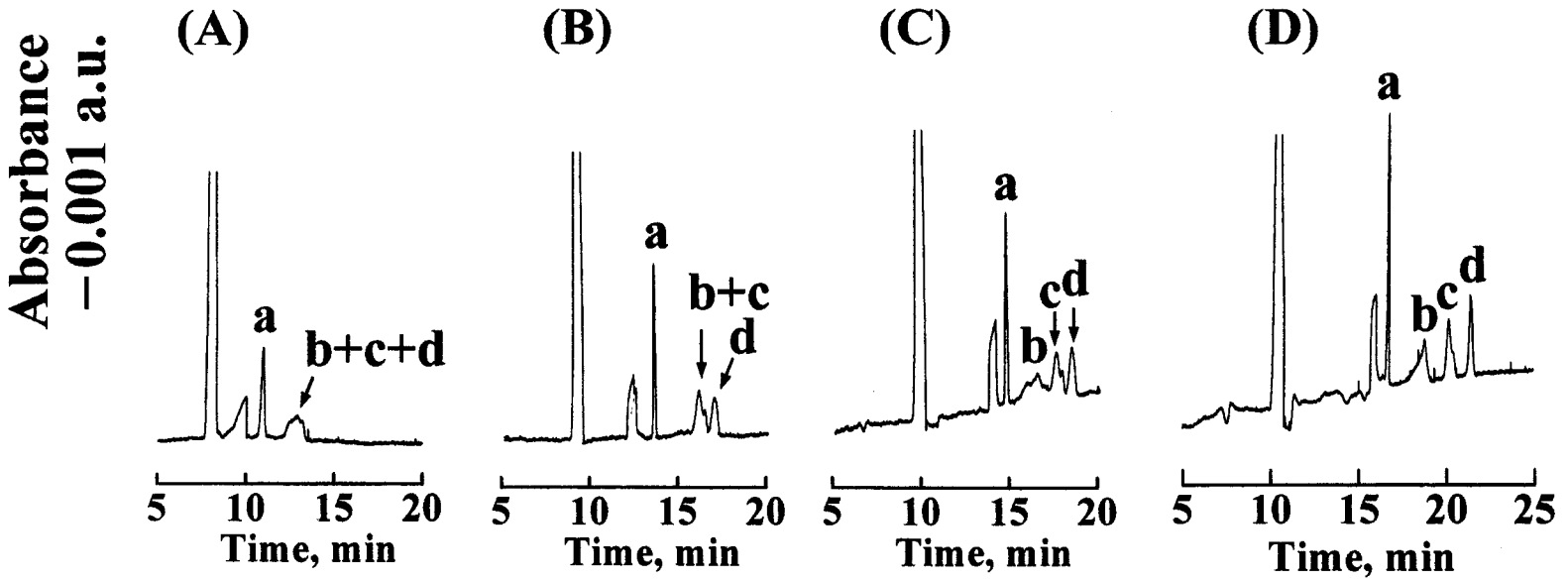

Figure 1. Electropherograms of a standard solution of phenol, PTPB, DPB, and MPB obtained with different BGE concentrations: (A) 20 mM, (B) 40 mM, (C) 50 mM, (D) 60 mM. CZE conditions: capillary, 50/72 cm × 75 μm ID; BGE, sodium tetraborate adjusted to pH 9.8 with 1 M NaOH; voltage, 15 kV; wavelength for detection, 200 nm. Sample, 1.0 mg L^{-1} of each analyte in artificial seawater; vacuum injection period, 4 s (84 nL). Peak identification: a, phenol; b, PTPB; c, DPB; d, MPB.

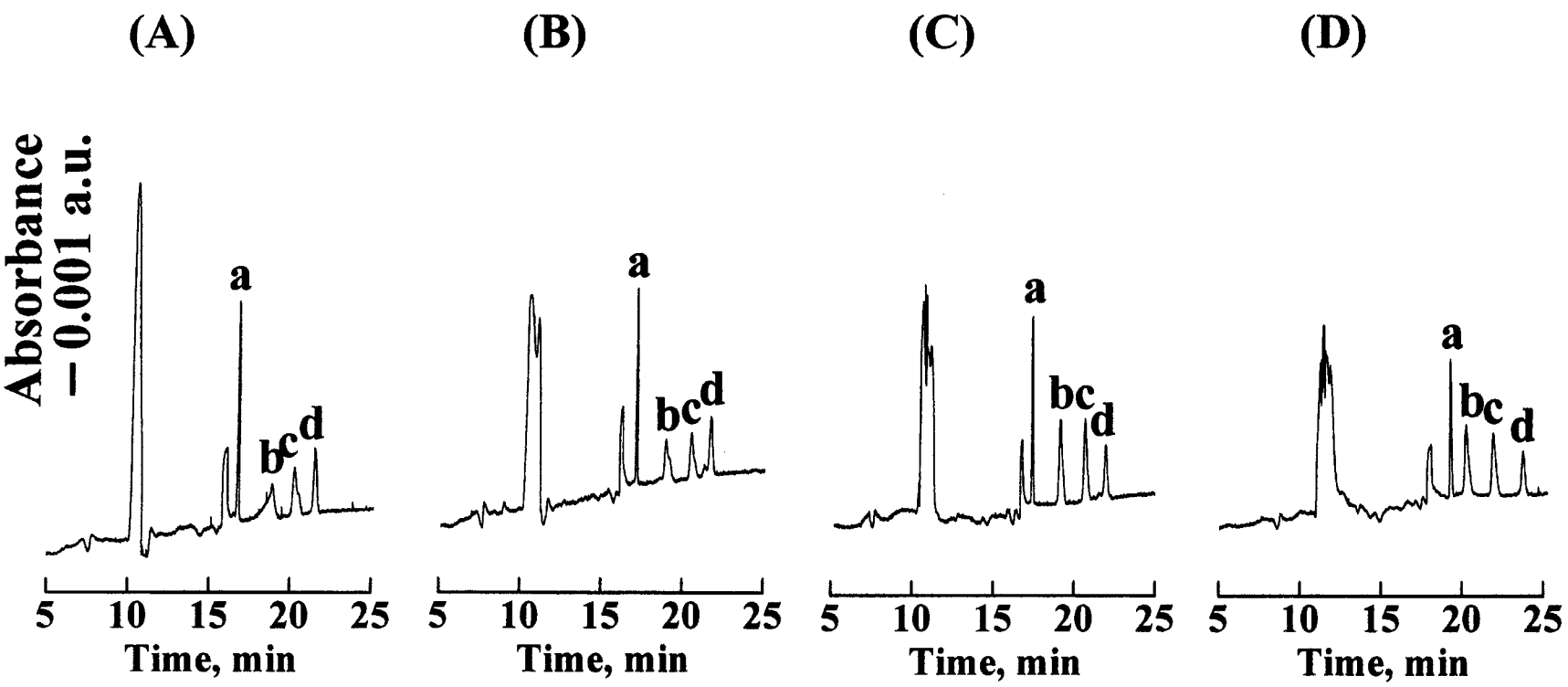

Figure 2. Electropherograms of a standard solution of phenol, PTPB, DPB, and MPB obtained with different ACN concentrations in the samples: (A) 0% (v/v), (B) 10% (v/v), (C) 20% (v/v), (D) 30% (v/v). BGE, 60 mM sodium tetraborate adjusted to pH 9.8 with 1 M NaOH. Sample, 1.0 mg L^{-1} of each analyte in artificial seawater. Peak identification: a, phenol; b, PTPB; c, DPB; d, MPB. Other CZE conditions are as in Figure 1.

3.3. Effect of the sample-injection time

The sample-injection time was varied between 2–6 s (results are not shown). Peak heights for PTPB, DPB, and MPB increased concomitantly with increasing injection time up to 4 s; then they decreased slightly. The peak height for phenol increased with the injection time up to 5 s; then it almost leveled off. The migration time increased concomitantly with increasing injection time. The maximum peak heights were obtained for PTPB, DPB, and MPB, except for phenol when the sample-injection time was 4 s. Therefore, 4 s was used further as the optimum sample-injection time.

3.4. Calibration graphs

Standard solutions for PTPB, DPB, MPB, and phenol were prepared using ASW containing 20% (v/v) ACN and 0.003% pyridine. Calibration graphs for all analytes were linear using both the peak area and peak height. Regression equations relating the area response to concentration for PTPB, DPB, MPB, and phenol (x, 0–1.5 mg L^{-1}) were $y = 3.94 \times 10^4 x + 9.20 \times 10^2$ (correlation coefficient, 0.9992), $y = 3.75 \times 10^4 x - 8.22 \times 10^2$ (0.9994), $y = 1.85 \times 10^4 x - 1.74 \times 10^2$ (0.9973), and $y = 2.84 \times 10^4 x + 9.52 \times 10^2$ (0.9983), respectively. Those relating the respective peak heights were $y = 2.83 \times 10^3 x + 8.42 \times 10^1$ (0.9967), $y = 2.64 \times 10^3 x - 2.07$ (0.9999), $y = 1.55 \times 10^3 x - 4.37$ (0.9976), and $y = 4.85 \times 10^3 x + 3.72 \times 10^2$ (0.9831). The LODs for PTPB, DPB, MPB, and phenol were, respectively, 55, 78, 126, and 30 μg L^{-1} at a signal-to-noise ratio of three. At the level of 0.5 mg L^{-1}, the RSDs (n=4) for the above analytes were in the respective ranges of 2.7–5.7, 0.68–6.1, and 0.69–1.1% for peak area, peak height, and migration time.

3.5. Degradation of pyridine-triphenylborane in artificial seawater

Results for degradation experiments are depicted in Fig. 3. In the open air, PTPB was degraded rapidly with 34% of the degradation ratio after one day, and disappeared after 15 days (Fig. 3a). Our results resemble those obtained by Zhou et al. [3]: 51% of PTPB were degraded under UV-A irradiation (50°C) after one day. Concentration of phenol increased to 0.57 mg L^{-1} after 30 days with decreasing concentration of PTPB. After 7 days, MPB peak appeared (0.16 mg L^{-1}), then decreased, and disappeared after 20 days. Figures 4(a), 4(b), and 4(c) respectively depict electropherograms of the sample solutions immediately after preparation, after 8, and 30 days. In a room with light, 25% of PTPB was degraded after one day. Then it was degraded slightly until 10 days. The concentration was almost constant until 30 days (Fig. 3b); 34% of PTPB were degraded after 30 days. Phenol was observed after 7 days. Its concentration increased gradually until 30 days (0.068 mg L^{-1}). In a room without light, 18% of PTPB was degraded after one day, then it was degraded slightly until 7 days, and the concentration was almost constant until 30 days (Fig. 3c); 25% of PTPB were degraded after 30 days, which was similar to results obtained by Zhou et al. [3]: 23% of PTPB degraded in ASW by hydrolysis. Phenol was observed after 10 days. Its concentration increased gradually until 30 days (0.037 mg L^{-1}). These results suggest that the effect of photolysis on the degradation of PTPB in ASW was stronger than that of hydrolysis. In no conditions was DPB observed.

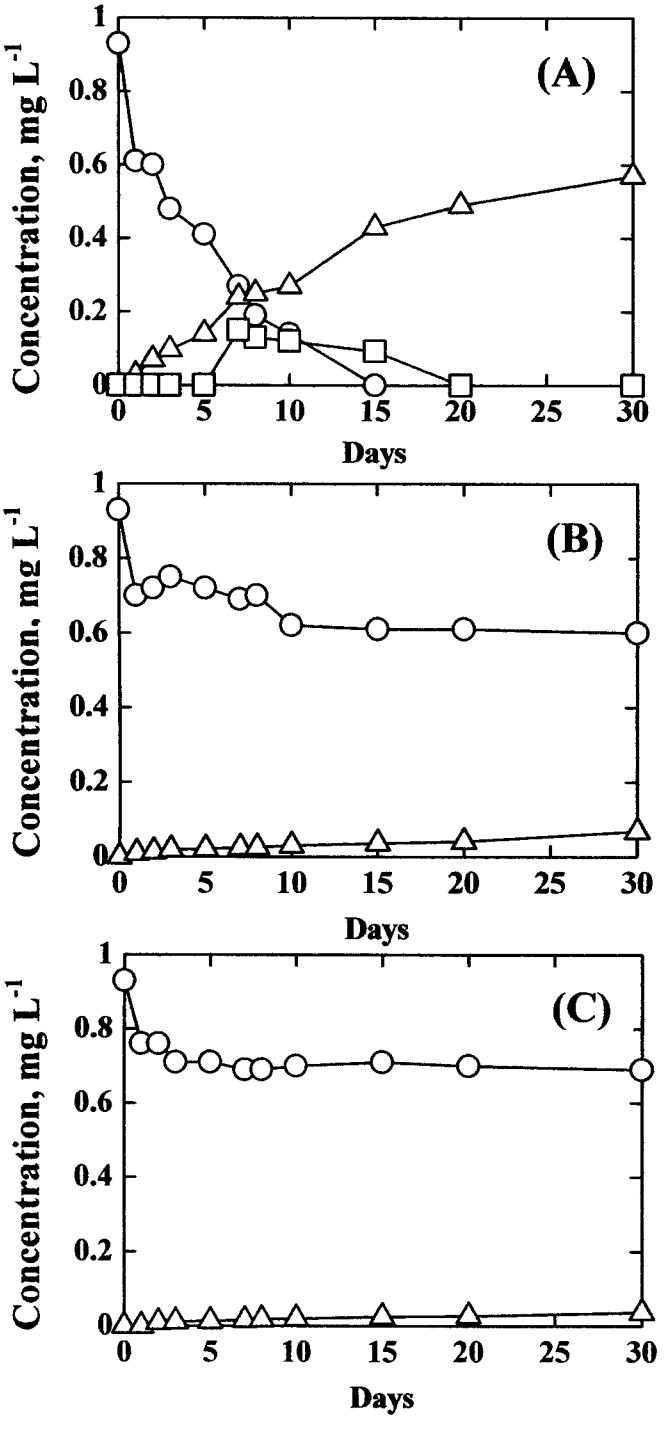

Figure 3. Degradation of PTPB and the formation of MPB and phenol in (A) the open air, (B) a room with light (25°C), and (C) a room without light (25°C). Sample: original sample, 1.0 mg L^{-1} PTPB in artificial seawater; samples used for analysis, 20% (v/v) ACN were added. Other CZE conditions are as shown in Figure 1. ○: PTPB; □: MPB; ▽: phenol.

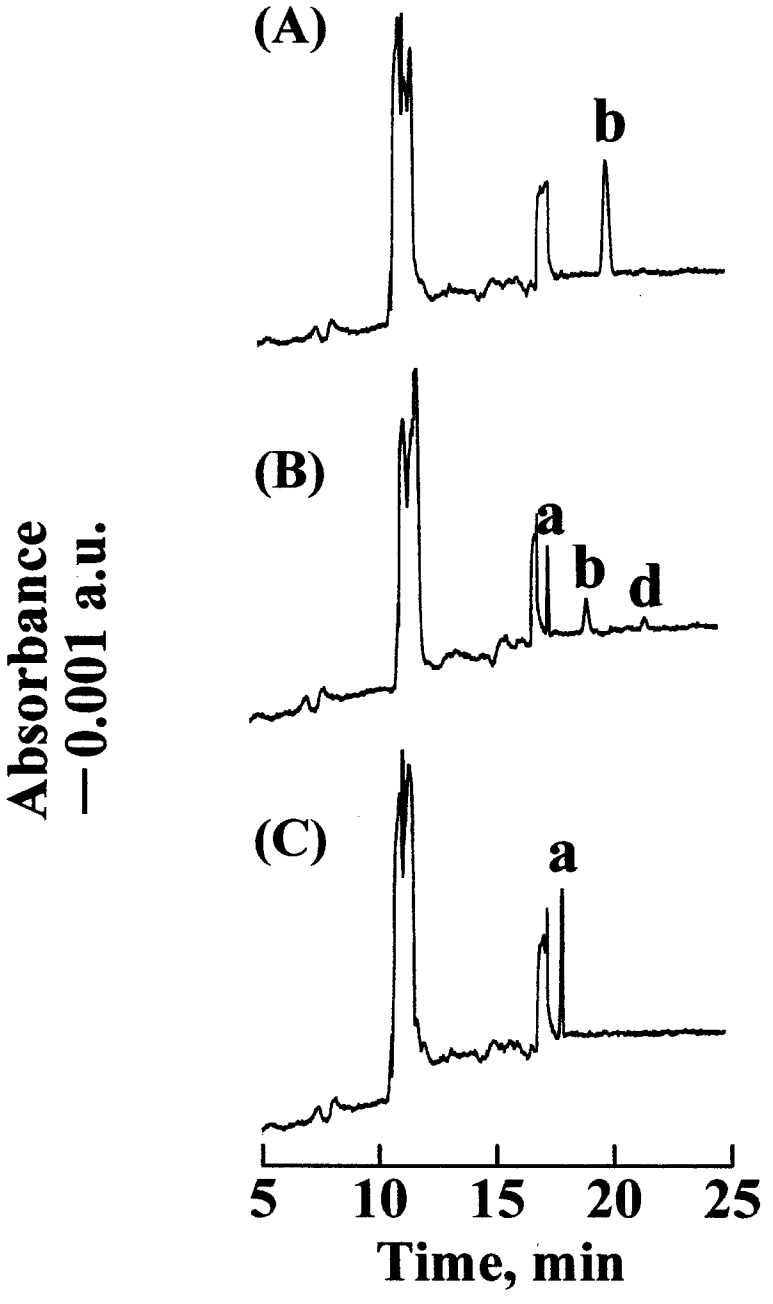

Figure 4. Electropherograms obtained in the degradation experiment for PTPB in the open air (on the rooftop): (A) sample, 1.0 mg L^{-1} PTPB in artificial seawater immediately after preparation containing 20% (v/v) ACN; (B) sample, collected after 7 days containing 20% (v/v) ACN; (C) sample, collected after 30 days containing 20% (v/v) ACN. Other CZE conditions and identification of peaks are as in Figure 1.

4. Conclusions

A capillary zone electrophoresis method was developed for the simultaneous determination of anti-fouling agent PTPB and its degradation products, DPB, MPB, and phenol in ASW with no extraction procedure. The ASW samples, in which 20% (v/v) acetonitrile (ACN) was added, were injected directly into the capillary using vacuum injection. As the background electrolyte (BGE), 60 mM sodium tetraborate adjusted to pH 9.8 was used. The proposed simple method provides sufficient detection power and precision to be useful for degradation experiments in ASW. The PTPB samples dissolved in ASW were put in the open air and rooms with and without light. We inferred that PTPB in ASW was more degraded by photolysis than by hydrolysis. The proposed CZE method has been demonstrated as a useful tool to elucidate the PTPB degradation process and its degradation products in ASW. Additional improvements of the LODs and examination of the effects of coexisting constituents in natural seawater are expected to make the method more useful.

References

1. Okamura, H., Kitano, S., Toyota, S., Harino, H., Thomas, K. V., *Chemosphere* 2009, *74*, 1275-1278.
2. Amey, R. L., Waldron, C., *In Proceedings of International Symposium on Antifouling Paint and Marine Environment, Tokyo* 2004, 234-243.
3. Zhou, X., Okamura, H., Nagata, S., *Chemosphere* 2007, *67*, 1904-1910.

4. Tsuboi, A., Okamura, H., *Bull. Soc. Sea Water Sci. Jpn.* 2012, *66*, 275-282.

5. Hanada, Y., Tanizaki, T., Koga, M., Shiraishi, H., Soma, M., *Anal. Sci.* 2002, *18*, 445-448.

6. Takahashi, K., Yoshikawa, E., Akiyama, M., Kitaori, K., Masuoka, S., *J. Jpn. Soc. Colour Mater.* 2005, *78*, 50-56.

7. Mochida, K., Onduka, T., Amano, H., Ito, M., Ito, K., Tanaka, H., *Mar. Pollut. Bull.* 2012, *64*, 2807-2814.

8. Fukushi, K., Yakushiji, Y., Okamura, H., Hashimoto, Y., Saito, K., *J. Chromatogr. A* 2010, *1217*, 2187-2190.

9. Kaewchuay, N., Yakushiji, Y., Fukushi, K., Saito, K., Hirokawa, T., *Electrophoresis* 2011, *32*, 1486-1491.

10. Kaewchuay, N., Fukushi, K., Tsubui, A., Okamura, H., Saito, K., Hirokawa, T., *Anal. Sci.* 2012, *28*, 1191-1196.

11. Okamoto, T., Fukushi, K., Takeda, S., Wakida, S., *Electrophoresis* 2007, *28*, 3447-3452.

12. Zhu, Q., Xu, X., Huang, Y., Xu, L., Chen, G., *J. Chromatogr. A* 2012, *1246*, 35-39.

13. Hruška, V., Jaroš, M., Gaš, B., *Electrophoresis* 2006, *27*, 984-991.

14. Kim, J.-B., Britz-McKibbin, P., Hirokawa, T., Terabe, S., *Anal. Chem.* 2003, *75*, 3986-3993.

15. Shihabi, Z. K., *Electrophoresis* 2002, *23*, 1612-1617.

Conclusions

In the present work, the purpose of this study is to develop a CZE procedure to enhance the sensitivity for simultaneous determination of PTPB and its degradation products: diphenylborinic acid (DPB), phenylboronic acid (MPB), and phenol. The results have been summarized here.

In general introduction, the purpose of the present study was described as well as the purpose of anti-fouling agent and the principle of capillary zone electrophoresis (CZE) used in this study throughout.

In Chapter 1, field amplified sample injection (FASI) was developed to enhance the sensitivity for the analytes and applied to the analysis of paint-waste samples. FASI is a popular and simple in-line sample concentration technique. The analytical conditions, such as time of water plug injection, time, and voltage of sample introduction were examined and optimized. Under the optimized conditions (injection time of the water plug, 2 s; sample injection, 5 kV for 6 s), the peak heights for PTPB and DPB using the FASI were, respectively, 16 and 58 times higher than those obtained using electrokinetic injection (EKI, 5 kV for 6 s). No peaks for MPB and phenol were observed using EKI. The results show that in-line sample concentration was performed for PTPB, DPB, MPB, and phenol using the FASI. The relative standard deviations (RSDs, $n = 4$) for the analytes listed above were in the respective ranges of 6.2 – 14, 5.9 – 10, and 0.49 – 0.62% for the peak area, peak height, and migration time. The limit of detections (LODs, at a *S/N* of 3) for PTPB, DPB, MPB, and phenol were, respectively, 0.85, 0.88, 44, and 28 $\mu g\ L^{-1}$. The LODs of PTPB and DPB were *ca.* 30 times lower than those for the vacuum injection procedure, but the LODs of MPB and phenol were similar to those for the vacuum

injection. The FASI-CZE procedure was applied to the determination of above analytes in paint wastes obtained from shipyards. The concentrations of PTPB, DPB, MPB, and phenol in the paint-waste samples were 0.076 – 0.53, 0.015 – 0.36, 1.7 – 22, and 1.2 – 13 $\mu g\ g^{-1}$, respectively.

In Chapter 2, a novel hybrid sample injection mode (HSIM) that presents the combination of EKI and vacuum injection was developed to enhance detection sensitivity in CZE. Samples were introduced using both vacuum and electrokinetic injections simultaneously, with a water plug injected into the capillary prior to sample introduction. Using a sample mixture of PTPB, DPB, MPB, and phenol dissolved in acetonitrile (ACN), time of water plug injection, time, and voltage of sample introduction were examined and optimized. Under the optimized conditions (injection time of the water plug, 1 s; sample injection, 4 kV for 4 s), signal intensity (peak height) was increased up to 30-fold in comparison with only vacuum injection for 4 s. The RSDs (n = 4, intra-day) for the above analytes were in the ranges of 1.9–11%, 4.3–9.2%, and 0.34–0.66% for peak area, peak height, and migration time, respectively. The LODs (at a S/N of 3) for PTPB, DPB, MPB, and phenol were, 0.88, 1.0, 21, and 23 μg/L, respectively. Using HSIM the LOD for MPB was *ca.* 2 times lower than the LOD for the FASI procedure, while the LODs for PTPB, DPB, and phenol were similar to those for the FASI procedure. The HSIM could be a simple and promising procedure to be useful for enhancing the sensitivity for both low- and high-mobility ions in CZE.

In Chapter 3, A capillary zone electrophoresis method was developed for the simultaneous determination of anti-fouling agent PTPB and its degradation products, DPB, MPB, and phenol in ASW with no extraction procedure. The ASW samples, in which 20% (v/v) acetonitrile (ACN) was added, were injected directly into the capillary

using vacuum injection. As the background electrolyte (BGE), 60 mM sodium tetraborate adjusted to pH 9.8 was used. The LODs (S/N=3) for PTPB, DPB, MPB, and phenol were, respectively, 55, 78, 126, and 30 $\mu g\ L^{-1}$. The proposed simple method provides sufficient detection power and precision to be useful for degradation experiments in ASW. The PTPB samples dissolved in ASW were put in the open air and rooms with and without light. We inferred that PTPB in ASW was more degraded by photolysis than by hydrolysis. The proposed CZE method has been demonstrated as a useful tool to elucidate the PTPB degradation process and its degradation products in ASW. Additional improvements of the LODs and examination of the effects of coexisting constituents in natural seawater are expected to make the method more useful.

These studies demonstrate that the proposed FASI, HSIM, and the CZE method without extraction procedure are simple and promising procedures to be useful for simultaneous determination of PTPB, DPB, MPB, and phenol. However, further works are still required to improve the sensitivity to analyze real environmental samples such as seawater. It is also necessary to investigate the effects of different kinds of constituents including organic substances dissolved in seawater.

List of Publications

1. **Chapter 1**

KAEWCHUAY Netnapit, FUKUSHI Keiichi, TSUBOI Ai, OKAMURA Hideo, et al.: Simultaneous Determination of Pyridine-Triphenylborane Anti-Fouling Agent and Its Degradation Products in Paint-Waste Sample Using Capillary Zone Electrophoresis with Field-Amplified Sample Injection. ANALYTICAL SCIENCES, 28, 1191-1196, 2012.

2. **Chapter 2**

KAEWCHUAY Netnapit, YAKUSHIJI Yuki, FUKUSHI Keiichi, SAITO Keiitsu, et al.: A novel hybrid mode of sample injection to enhance CZE sensitivity for simultaneous determination of a pyridine-triphenylborane anti-fouling agent and its degradation products. Electrophoresis, 32, 1486-1491, 2011.

3. **Chapter 3**

KAEWCHUAY Netnapit, FUKUSHI Keiichi: Simultaneous Determination of Pyridine-Triphenylborane Anti-Fouling Agent and Its Degradation Products in Artificial Seawater Using CZE. Chromatographia, manuscript in preparation.

Acknowledgements

The author expresses her deep gratitude to Dr. Keiichi Fukushi for his continuing kind guidance and encouragement on this thesis.

The author would like to thank Prof. Dr. Takeshi Hirokawa, Dr. Hideo Okamura, Dr. Keiitsu Saito, Dr. Takeshi Nakano, and Dr. Masayoshi Okubo for their kind advice, useful suggestions and encouragement.

The author also would like to express her gratitude to The Rajamangala University of Technology Thanyaburi, Thailand for the scholarship support.

Finally, the author would like to express her family for support, understanding and encouragement.